

# **SELECTION OF A PRECIPITATION MODEL FOR USE IN THE NEW MEXICO STATEWIDE WATER ASSESSMENT**

By

Steve Walker, Author and GIS Coordinator

Thomas Schmugge, Remote Sensing Consultant

Ian Hewitt, Research Assistant

Ken Peterson, Hydrologic Technician

New Mexico Water Resources Research Institute

TECHNICAL COMPLETION REPORT

–

July 2016

The research on which this report is based was financed by the National Science Foundation through the New Mexico Experimental Program to Stimulate Competitive Research and the State of New Mexico through the New Mexico Water Resources Research Institute and New Mexico State University.

## **DISCLAIMER**

The New Mexico Water Resources Research Institute and affiliated institutions make no warranties, express or implied, as to the use of the information obtained from this data product. All information included with this product is provided without warranty or any representation of accuracy and timeliness of completeness. Users should be aware that changes may have occurred since this data set was collected and that some parts of these data may no longer represent actual conditions. This information may be updated without notification. Users should not use these data for critical applications without a full awareness of its limitations. This product is for informational purposes only and may not be suitable for legal, engineering, or surveying purposes. The New Mexico Water Resources Research Institute and affiliated institutions shall not be liable for any activity involving these data, installation, fitness of the data for a particular purpose, its use, or analyses results.

## **ACKNOWLEDGEMENTS**

Dr. Sam Fernald, Professor and Director, New Mexico Water Resources Research Institute, New Mexico State University

Mike Halbleib, GIS Specialist and Research Assistant, PRISM Climate Group, Oregon State University

Dr. Jan Hendrickx, Professor of Hydrology, Department of Earth and Environmental Science, New Mexico Institute of Mining and Technology

Dr. Marcy Litvak, Associate Professor, Department of Biology, University of New Mexico  
Francisco Ochoa, GIS Technician, New Mexico Water Resources Research Institute, New Mexico State University

Dave Thatcher, Supervisory Range Technician, USDA-ARS, Jornada Experimental Range

# TABLE OF CONTENTS

<b>1. Introduction</b>	<b>1</b>
1.1. Innovation Working Group	1
1.2. Project Proposal	1
1.3. Report Structure	4
<b>2. Study Area</b>	<b>5</b>
2.1. Model Processing and Verification Study Area	5
2.2. Model Dissemination Study Area	5
<b>3. Phase One Process – Model Collection, Processing and Preliminary Comparison</b>	<b>7</b>
3.1. Methodology	7
3.1.1. Model Data Collection	7
3.1.1.1. Advanced Hydrologic Prediction Service (AHPS)	9
3.1.1.2. Climate Hazards Group InfraRed Precipitation with Station data (CHIRPS)	10
3.1.1.3. Precipitation Estimation from Remotely Sensed Information Using Artificial Neural Networks (PERSIANN)	11
3.1.1.4. Parameter-elevation Relationships on Independent Slopes Model (PRISM)	12
3.1.1.5. Tropical Rainfall Measuring Mission (TRMM)	13
3.1.2. Model Processing and Visualization	14
3.1.3. Model Statistics	14
3.2. Results	15
3.2.1. Model Visualization and Spatial Analysis	15
3.2.2. Statistical Analysis	21
3.2.3. Precipitation Model Advantages and Disadvantages	25
<b>4. Phase Two Process – Verification and Validation</b>	<b>27</b>
4.1. Methodology	27
4.1.1. Field Data Collection	27
4.1.1.1. Rain Gauges of the Jornada Experimental Range	27
4.1.1.2. Rain Gauges of the Sevilleta National Wildlife Refuge	30
4.1.1.3. Rain Gauges of the AmeriFlux Energy Flux Network	30
4.1.2. Model Data Extraction	31
4.1.3. Model Comparison	31
4.2. Model Comparison Results	32
<b>5. Phase Three Process – Quality Control</b>	<b>33</b>
5.1. Methodology	33
5.1.1. PRISM High Resolution Model Acquisition	33
5.1.2. Verification of the PRISM M2/D1 High Resolution Model	33
5.1.3. Verification of the PRISM M3/D2 High Resolution Model Revision	36
5.2. PRISM M3/D2 High Resolution Revision Results and Conclusion	38
<b>6. Phase Four – Precipitation Component Data Dissemination</b>	<b>40</b>
6.1. Continuing Forward with Precipitation Component Data Dissemination	40
<b>7. References</b>	<b>41</b>
<b>Appendix A – Definitions</b>	<b>44</b>

## LIST OF TABLES

<b>TABLE 1.</b> Data Descriptions of Precipitation Models	8
<b>TABLE 2.</b> Water Assessment Component Model Comparisons	22
<b>TABLE 3.</b> Precipitation Model Advantages and Disadvantages	26
<b>TABLE 4.</b> List of Rain Gauges Used for Validation and Verification of Precipitation Products	28

## LIST OF FIGURES

<b>FIGURE 1.</b> 2013 New Mexico Water Conference Poster	2
<b>FIGURE 2.</b> Preliminary Study Area	5
<b>FIGURE 3.</b> New Mexico Headwaters Study Area	6
<b>FIGURE 4.</b> AHPS Model Yearly Spatial Results	16
<b>FIGURE 5.</b> CHIRPS Model Yearly Spatial Results	17
<b>FIGURE 6.</b> PERSIANN Model Yearly Spatial Results	18
<b>FIGURE 7.</b> PRISM Model Yearly Spatial Results	19
<b>FIGURE 8.</b> TRMM Model Yearly Spatial Results	20
<b>FIGURE 9.</b> Water Assessment Component Models Graphic Display	23
<b>FIGURE 10.</b> 2007 Wet Year Model Histogram Comparison	24
<b>FIGURE 11.</b> 2012 Dry Year Model Histogram Comparison	25
<b>FIGURE 12.</b> Location of Rain Gauges for Validation and Verification of Precipitation Products	29
<b>FIGURE 13.</b> Correlation Between Precipitation Models and Jornada ER Rain Gauges	32
<b>FIGURE 14.</b> 4-kilometer PRISM M2 Precipitation Data at Jornada ER, Aggregated for Year 2008	34
<b>FIGURE 15.</b> 800-meter PRISM M2 Precipitation Data at Jornada ER for July 2008	35
<b>FIGURE 16.</b> 800-meter PRISM D1 Precipitation Data at Jornada ER, Aggregated for July 2008	35
<b>FIGURE 17.</b> 800-meter PRISM M2 Correlation with New Mexico Precipitation Stations	37
<b>FIGURE 18.</b> 800-meter PRISM Monthly D1 Aggregation Correlation with NM Precipitation Stations	38
<b>FIGURE 19.</b> 800-m PRISM M3 Correlation with NM Precipitation Stations	39
<b>FIGURE 20.</b> Dynamic Statewide Water Budget Estimator	40

## 1.0 INTRODUCTION

### 1.1 Innovation Working Group

On November 17-19, 2013 at the Santa Ana Pueblo, a workshop called the New Mexico Statewide Water Budget Innovation Working Group collaborated on ideas and planning strategies for generating a working statewide water budget that supports water resource sustainability and improves the future of sustainable energy development. This workshop, funded by the third New Mexico Experimental Program to Stimulate Competitive Research (NM EPSCoR III, Appendix A), brought together community and government water managers, scientists, experts, and researchers in the fields of hydrology, geology, geohydrology, civil engineering, water planning, remote sensing, geography, and meteorology to set the stage for a number of project activities. The day and a half long set of discussions determined the information and data which are available or needed for the project, the deliverables and structures required for the project, and the best practices for crafting a water budget that accomplished the following set of objectives.

- 1) Support connections to energy, humans, and the environment in a Social / Natural Science Nexus (a division of the overall EPSCoR IV team – others teams include the BioAlgal Energy Development, the Solar Energy Development, the Osmotic Power Development, the Uranium Transport and Site Remediation, and the Geothermal Energy Resources and Sustainability).
- 2) Involve stakeholders (i.e. acequia, pueblo, city, and irrigation management, relict groundwater users, etc.) in decision making processes.
- 3) Incorporated datasets from other projects.
- 4) Complement the New Mexico Office of the State Engineer (NMOSE) programs within frameworks that they support.
- 5) Provide useful data for planning and policy.

The Innovation Working Group provided a clear understanding of the purpose and intended use of a statewide water budget (later termed “assessment”, Appendix A) and a system that would be appropriate for determining water appropriation availability and impairment.

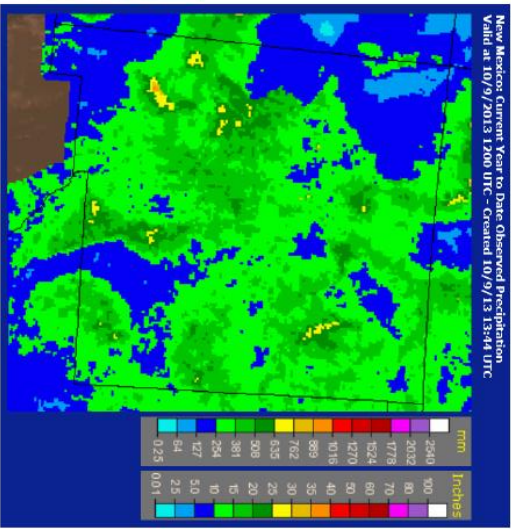
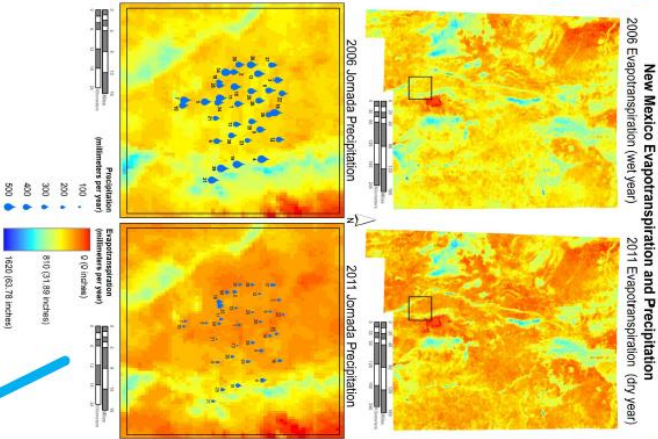
### 1.2 Project Proposal

During the Innovation Working Group and later planning phases, many available datasets were being used to display the planning of the water budget process. For the 2013 New Mexico Water Conference (Appendix A), one of the first posters (Figure 1) designed to herald the work for this project depicted all of the components together in a single illustration, along with component data that had been acquired at the time. This poster served as an overview of the different components that were researched by the different water assessment teams.

# Ongoing Statewide Water Budget Research for EPSCoR Funding

**Evapotranspiration estimates from a MODIS satellite surface temperature model**

Present research is aimed at validating the evapotranspiration model. So far the model estimates the movement of between 100 and 150 million acre-feet of water within the New Mexico boundary.



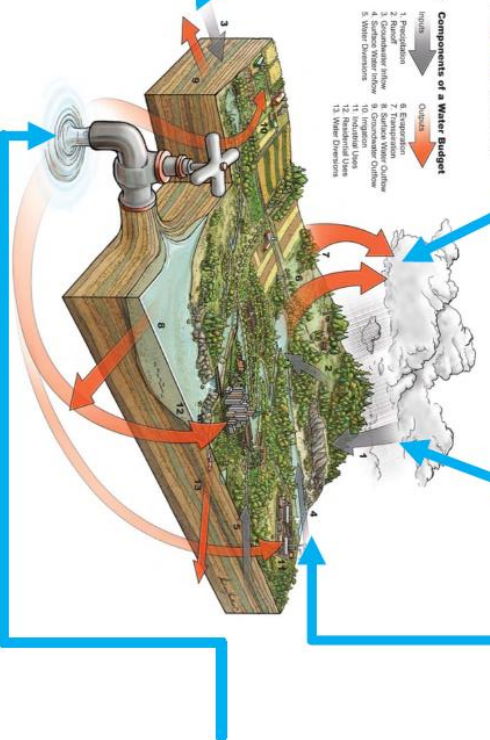
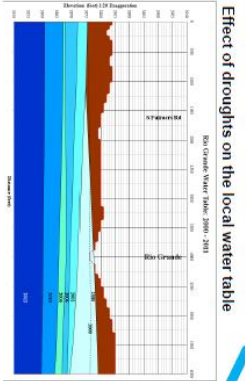
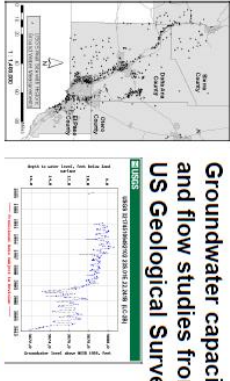
Precipitation estimates from rain gauge interpolation and direct radar coverage data from the National Weather Service

Evapotranspiration and Precipitation are the major movers of water in New Mexico and the main components of the state's water budget.

**Surface Water Flow Statistics from the US Geological Survey**



**Groundwater capacities and flow studies from the US Geological Survey**



**Water Use Statistics from the NM Office of the State Engineer**

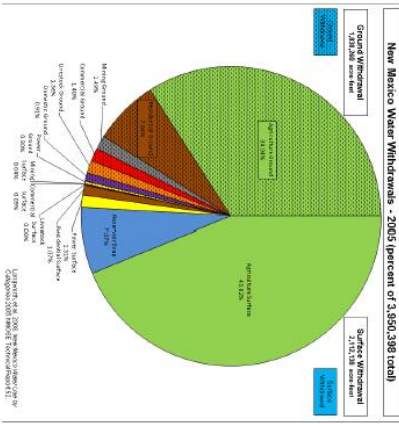


**Figure 1.** 2013 New Mexico Water Conference Poster. (Upper Illustrations: Jornada Experimental Range rain data displayed on the SSEBop ET model and the AHPs Precipitation model.)

From desert sands to alpine forests and from river valleys to mountainous peaks, New Mexico possesses several different environments and a variety of elevations. The arid climate of New Mexico explains why precipitation and evapotranspiration (Appendix A) are the largest movers of water in the state. At wetter times, each flux moves more than 100 million acre-feet of water per year to and from the ground. A Precip/ET group was formed early in the project and responsible for quantifying the precipitation / evapotranspiration components accurately through the use of a variety of remotely sensed (Appendix A) datasets. The group gathered together a number of models for each component to compare against one another in order to determine which one was the most accurate for the state of New Mexico. Four phases were originally proposed at the beginning of fiscal year 2014 (July 1) that accuracy assessed the component models against a high resolution evapotranspiration model that had been calibrated to the Rio Grande riparian corridor. This idea was dropped a few months later in favor of comparing the models against field measurements from rain gauges and evapotranspiration flux towers from many environments and elevations around New Mexico. The following four phases outline the acquisition, verification, quality control and dissemination of the component datasets worked on by the Precip/ET group.

**Phase One – Data Collection and Performance:** Obtain and compile all data and base

literature for a variety of precipitation and evapotranspiration models. Compare and contrast all data and produce tabular itemizations for basic statistical analyses for the entire state, for each year, for each model. Produce comparison graphs, histograms (Appendix A), and spatial displays for each model and consider the spatial and temporal scales of each product.

**Phase Two – Data Verification and Validation:** Validate each product against reliable

measurements. Obtain and compile all data and base literature for each validation model or dataset. Produce correlation scatter plots (Appendix A) that compare each validation product with each precipitation and evapotranspiration product. Establish one or two precipitation and evapotranspiration products to focus on as key products and that will require less model manipulation for further verification.

**Phase Three – Data Quality Control:** Fine tune and quality control the chosen precipitation

and evapotranspiration products to predict component values as precisely and accurately as possible for the unique environment of New Mexico. Make adjustments to the chosen component model and validate results to the greatest degree possible.

**Phase Four – Data Dissemination:** Compile all precipitation and evapotranspiration data into a geodatabase (Appendix A) and set of map documents at the spatial and temporal scale that will allow them to be combined with other water balance component data. Provide all pertinent metadata (Appendix A).

### **1.3. Report Structure**

Since in New Mexico the evapotranspiration component removes 85 to 90 percent of the precipitation component, the first two phases of the precipitation and evapotranspiration components proceeded hand in hand and utilized results from each to determine a baseline to compare all datasets. However, this report explains only the selection of the precipitation component. The selection of the evapotranspiration component is found elsewhere.

This document details the first three phases of the selection and improvement process for the precipitation component. The fourth phase is still in construction and will be reported on when the final data dissemination goes live. Each phase had a final outcome that carried to the next phase, therefore the methodology and results will be described for each phase individually before moving on to the next phase.

## 2.0 STUDY AREA

### 2.1 Model Processing and Verification Study Area

When starting the project, the preliminary study area (Figure 2) was the administrative border of the state of New Mexico. The exact area was well known and geospatial boundaries were already complete and easy to acquire. The first phase relied heavily on this study area since the variety of resolutions from the eight models (five precipitation and three evapotranspiration) provided many average depth values that had to be multiplied by the same area to compare them. Since the project looked for components for a *statewide* water assessment, the state boundary was the most logical choice. The temporal study time covered the year 2000 to the year 2013.



New Mexico is the fifth largest state in the United States, encompassing a total area of 121,589 square miles (315,194 square kilometers, 77,886,134 acres).

**Figure 2.** Preliminary Study Area.

### 2.2 Model Dissemination Study Area

After the project gained some ground, it was agreed that all areas outside of the state that had some degree of water entering the state should be included in the final clipping boundaries to take these additions and subtractions to the water budget into account. All of the subbasin hydrologic units (HUC8, see Appendix A) that have some portion of their runoff entering New Mexico were included in the final boundary product termed the New Mexico Headwaters study area (Figure 3).

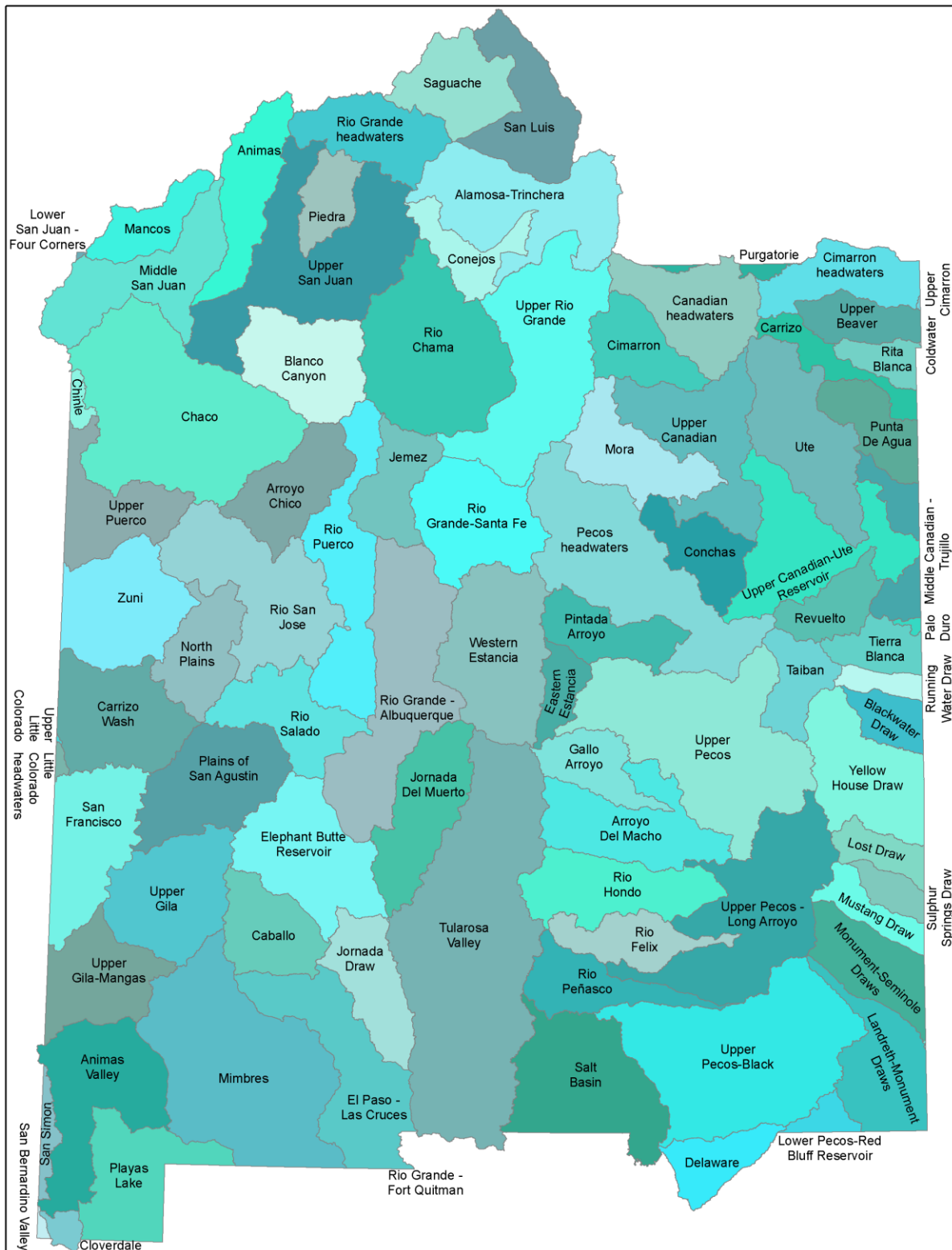


Figure 3. New Mexico Headwaters Study Area.

### 3.0 PHASE ONE PROCESS

#### 3.1 Methodology – Model Collection, Processing and Preliminary Comparison

##### 3.1.1 Model Data Collection

Five criteria were used in selecting the precipitation component models considered for this project. 1) Was the model publicly available? 2) Was the model temporally continuous and in use at the present time? 3) Was the model spatially continuous over the entire state and able to be subdivided into units as small as a HUC8 subbasin? 4) Did the model provide quantifiable precipitation values that could be used or converted for use in a water budget? 5) Was there suitable academic background to describe the process for the model and allow it to be adjusted to New Mexico's unique environment?

Those questions resulted in the selection of the following five precipitation models: the *Advanced Hydrologic Prediction Service* (AHPS) from the National Oceanic and Atmospheric Administration (NOAA), the *Climate Hazards Group InfraRed Precipitation with Station* (CHIRPS) from the University of California - Santa Barbara (UCSB), the *Precipitation Estimation from Remotely Sensed Information using Artificial Neural Networks* (PERSIANN) from the University of Arizona (UofA), the *Parameter-elevation Relationships on Independent Slopes Model* (PRISM) from Oregon State University (OSU), and the *Tropical Rainfall Measuring Mission* (TRMM) from the National Aeronautics and Space Administration (NASA) and the Japan Aerospace Exploration Agency (JAXA).

The most notable differences between the precipitation model data (Table 1), were the methods used to apply values to each pixel, the spatial resolution (area) of the pixels or spacing of data points, the coverage (global or continental) of the entire model, the file formats and the ease of acquisition. These differences required the model data to be standardized for the final results for the first phase. All component models needed to be clipped to the preliminary study area and provide a continuous geographic coverage of it over a one-year temporal time period. The methods are explained in the individual model descriptions. Model datasets were collected and processed at the same time as the literature that explained their creation and use from inception to finish.

	Abbreviation	Creator	Spatial Resolution	Temporal Resolution	Model Method	File Format	Raw Data Location	
	<b>AHPS</b>	Advanced Hydrologic Prediction Service	National Oceanic and Atmospheric Agency, National Weather Service	4 km	Daily, Monthly, Yearly	<b>PRISM with NEXRAD radar</b> bias east of the continental divide	Shapefile (SHP), Network Common Data Form (NetCDF)	<a href="http://water.weather.gov/precip/download.php">http://water.weather.gov/precip/download.php</a>
	<b>CHIRPS</b>	Climate Hazards Group InfraRed Precipitation with Station data	University of California - Santa Barbara, Climate Hazards Group	0.05° ~ 5 km	Monthly	<b>Satellite</b> imagery with in-situ station data	Band Interleaved by Line (BIL), Tagged Image File Format (TIFF)	<a href="ftp://chg-ftpout.geog.ucsb.edu/pub/org/chg/products/CHIRPS-latest/">ftp://chg-ftpout.geog.ucsb.edu/pub/org/chg/products/CHIRPS-latest/</a>
	<b>PERSIANN</b>	Precipitation Estimation from Remotely Sensed Information using Artificial Neural Networks	University of Arizona, Hydrology and Water Resources Department	4 km	Daily	Geostationary <b>satellite</b> longwave infrared imagery	Binary (BIN)	<a href="http://chrs.web.uci.edu/persiann/">http://chrs.web.uci.edu/persiann/</a>
	<b>PRISM</b>	Parameter-elevation Relationships on Independent Slopes Model	Oregon State University and United States Department of Agriculture	4 km & 800 meter (with fee)	Daily, Monthly, Yearly	Climatologic- <b>Aided Interpolation</b> (CAI)	BIL, ASCII	<a href="http://prism.oregonstate.edu/recent/">http://prism.oregonstate.edu/recent/</a>
	<b>TRMM</b>	Tropical Rainfall Measuring Mission	National Aeronautics and Space Administration and Japan Aerospace Exploration Agency	0.25° ~ 22 km	3-Hour, 10-Day, Monthly, Yearly	Real-time TRMM Multi- <b>Satellite</b> Microwave Radiometer Analysis	BIN, TIFF, Giovanni, GDS, NetCDF, OPeNDAP, Keyhole Markup Language (KML), Graphics Interchange Format (GIF), Portable Network Graphics (PNG)	<a href="http://pmm.nasa.gov/data-access/downloads/tmm">http://pmm.nasa.gov/data-access/downloads/tmm</a>

**Table 1.** Data Descriptions of Precipitation Models.

### 3.1.1.1. Advanced Hydrologic Prediction Service (AHPS)

The implementation of weather radar provides real-time observed rainfall data for hydrologic forecasting, but direct use is unacceptable due to a variety of errors associated with the radar observations (Wilson and Brandes 1979, Austin 1987, Smith et al. 1995, Fread et al. 1995). Radar sampling errors occur due to freezing or frozen precipitation; low topped convection; bright banding; accuracy of reflectivity to rainfall relationship; and radar calibration, location, elevation, range degradation or coverage (Lawrence et al. 2003). To correct radar errors and improve accuracy, the AHPS Gridded Observed Precipitation Dataset uses a factor that corrects bias (Appendix A) at hourly intervals from the precipitation estimates from the Weather Service Radar 1988 Next-Generation Doppler Radar (WSR-88D NEXRAD) to combine over 10,000 precipitation gauges scattered across the country into a single multi-sensor package (Seo 1999). In areas uncovered by radar, such as the mountainous territory west of the Continental Divide, gauge reports are correlated to long term PRISM climatologic precipitation data and derived amounts are interpolated (Appendix A) between gauge locations (National Climatic Data Center 2014). This product is primarily used for timely, high resolution precipitation prediction, but it is not perfect since precipitation gauges are associated with a number of errors as well. Gauge sampling errors occur from freezing precipitation, wind, gauge sites and obstructions, tipping bucket gauge errors during high intensity precipitation, and gauge maintenance (Lawrence et al. 2003). The NWS has persistent quality control issues and significant sampling errors can be present in monthly products (Lawrence et al. 2003).

The AHPS product was processed at twelve Continental United States River Forecast Centers (CONUS RFC) and was not provided as a raster image like the other precipitation models, but in a gridded field of precipitation values in polygons about 4 square kilometers in size. These data come in 24-hour totals starting at 1200 Greenwich Mean Time and are available from the beginning of 2005 to present.

### **3.1.1.2. Climate Hazards Group InfraRed Precipitation with Station data (CHIRPS)**

In 1999, scientists from the U.S. Geological Survey (USGS) and University of California, Santa Barbara (UCSB) began working on drought monitoring efforts in Africa through the U.S. Agency for International Development (USAID) Famine Early Warning Systems Network (FEWS NET). The early research focused on combining models of terrain-induced precipitation enhancement (Funk and Michaelsen 2004) with interpolated station data (Funk et al. 2003) to support the creation of standardized precipitation index maps (Husak et al. 2007) for African climate forecasts and their first drought analyses (Funk et al. 2005, Verdin et al. 2005). Since then, the index maps were combined with U.S. satellite resources, station precipitation averages, and rainfall predictors (elevation and location) to create the Climate Hazards Precipitation Climatology (CHPClim) dataset (Janowiak et al. 2001, Funk et al. 2007, Funk and Verdin 2010, Knapp et al. 2011, Funk et al. 2012). These improved monthly means are divided into months of 6-pentads (5 days) and multiplied by a bias removing factor created through a local regression (Appendix A) between the Tropical Rainfall Measuring Mission (TRMM) (Huffman et al. 2007, Huffman et al. 2011) dataset and the percentage of time during the pentad that cold cloud tops ( $<235^{\circ}$  K) were detected using quasi-global geostationary thermal infrared satellite observations to get units of millimeters per pentad (CHIRP) (Funk et al. 2014). Finally, the set of U.S. interpolated stations data are distance weighted and combined with the CHIRP data to produce the final product (Funk et al. 2014). Missing or incomplete infrared satellite coverage data gaps are filled using bias corrected atmospheric model rainfall fields from the NOAA Climate Forecast System, version 2 (CFSv2) (Saha et al. 2010, Environmental Modeling Center 2011).

The CHIRPS product was used as a  $0.05^{\circ}$  (approximately 5 kilometer) geotiff raster (Appendix A) and can be downloaded for all areas across the globe. The data has been aggregated and disaggregated into daily, monthly and yearly sets and covers a time period from the beginning of 1981 to present.

### **3.1.1.3. Precipitation Estimation from Remotely Sensed Information Using Artificial Neural Networks - Cloud Classification System (PERSIANN-CCS)**

In 1997, the Hydrology and Water Resources Department of the University of Arizona began work on a method to determine global distribution of rainfall through the use of conventional rain gauges, ground-based radar, infrared satellite imagery and the computational power and flexibility of an adaptive Artificial Neural Network (ANN) (Hsu et al. 1997, 1999, Sorooshian et al. 2000, 2005). This method was used to extract and combine information about these data and provide near real-time results and cover areas where data is sparse or non-existent, even over oceans. (Hsu et al. 1997, 1999, Sorooshian et al. 2000, 2005). The finished algorithm (Appendix A) begins with a continuous sampling of precipitation values estimated from infrared satellite data collected by the Geostationary Operational Environmental Satellite (GOES), associating a number of cloud texture patterns within the data to surface rainfall rates, and merges it with sparsely-sampled, high-quality, passive microwave precipitation estimates from TRMM, NOAA and the Defense Meteorological Satellite Program (DMSP) to create a global precipitation estimate (Hsu et al. 1997, 1999, Sorooshian et al. 2000, 2005). Calibration and quality control are performed by the adaptive training algorithm model that detects sampling errors in the satellite data with WSR-88D NEXRAD through a feedback loop and updates the retrieval parameters when new microwave observations become available at about 3 hour intervals (Sorooshian et al. 2000, 2005). The original ANN model was created and calibrated for use in tropical regions, such as Japan and Florida (Hsu et al. 1997, 1999). The model has since been introduced to areas with a variety of environments (United States, Mexico and Australia) with the conclusion that it shows promise, but requires improvement and remains under development (Sorooshian et al. 2000, 2005, Hong et al. 2004, 2007).

PERSIANN is a near-global product, providing coverage from 50°N to 50°S with a 0.04° to 0.25° (about 4 to 22-kilometer) spatial resolution and covers the time period from March of 2000 to present day in 30 minute, 1, 3 and 6-hour, and daily increments. The data are compressed into large raw datasets of specialized 4-byte binary float data (SUN system: big-endian) that describe the location of the anchor points and the numerical values in millimeters per pixel per time unit.

#### **3.1.1.4. Parameter-elevation Relationships on Independent Slopes Model (PRISM)**

In 1991, a research team led by Chris Daly, a Ph.D. student at Oregon State University, wrote an algorithm program that mimicked the tedious and time-consuming thought processes that expert climatologists use to create climate maps. Elevation at mountains and coastlines were known to be one of the main contributors to precipitation patterns, but the relationship between precipitation and elevation did not predict accurately across all landscapes, because areas of similar elevation on different sides of mountains can have very different precipitation. (Daly, Neilson and Phillips 1993; Daly, Taylor and Gibson 1997; Daly 2013). The PRISM method starts with the elevation from the locations of a variety of precipitation stations plotted against a 3-arcsec (about 80-m) resolution National Elevation Database digital elevation model (DEM, Appendix A) and a calculation for an algorithm based on the slope orientation (N, NE, E, etc.) of each DEM/station grid cell facet (Daly, Neilson and Phillips 1993; Daly, Taylor and Gibson 1997; University of Oregon 2015). The algorithm is further processed into a precipitation-DEM elevation regression function and prediction interval using detrended kriging (Appendix A) of values from nearby rainfall stations and weights the regression based on proximity to coastlines, location of temperature inversions and cold air pools, and several measures of terrain complexity (Daly, Neilson and Phillips 1993; Daly, Taylor and Gibson 1997; Daly 2013). This interpolated, gridded, precipitation estimate is finally collected into a time series (Appendix A) dataset using a method, called climatologically-aided interpolation (CAI, Appendix A), that looks at recurring patterns of mean local precipitation over decades of time, instead of elevation statistics (Daly 2013, University of Oregon 2015).

PRISM covers the North American Continent and provides estimates of precipitation, dew point, and minimum and maximum temperature and vapor pressure deficit at 0.042° and 0.0083° (4-kilometer and 800-meter) resolutions. The 800-meter resolution datasets require a fee, while the 4-kilometer datasets are free for download. Due to the CAI time series element of the model, the datasets cover periods from January 1895 to present and come in daily, monthly and yearly temporal resolutions. The yearly data format used in this phase of the study were geotiffs.

### **3.1.1.5. Tropical Rainfall Measuring Mission (TRMM)**

The experimental concept for TRMM was first proposed at the National Aeronautics and Space Administration (NASA) in 1984 to understand and predict 1) global energy, water cycles and mechanisms of global rainfall influence from tropical latent heating distribution; 2) the onset and development of the El Niño, Southern Oscillation (Appendix A); 3) the effect that rainfall has on the ocean thermohaline (Appendix A) circulations; and 4) to evaluate a space-based system for rainfall measurements (Kummerow et al. 2000). The Japan Aerospace Exploration Agency (JAXA) joined the initial study for the TRMM mission in 1986 and provided the world's first space-borne Precipitation Radar (PR) package and the H-II launch vehicle, while the U.S. provided the observatory, the TRMM Microwave Imager (TMI), a visible infrared scanner (VIRS), a lightning image sensor (LIS), a Clouds and Earth Radiant Energy System (CERES), and the satellite operation systems (JAXA 2007). TRMM was launched from the Tanegashima Space Center in November of 1997 and was deactivated on April of 2015 (reentered atmosphere in June), providing over seventeen years of data, even though the satellite was only designed for a lifetime of three years (JAXA 2007). The great success of TRMM comes from the complementary nature of its passive and active sensor instruments (allowing view of cloud-precipitation structures in three dimensions and determining rates, quantities, distributions of and correlations between rainfall, lightning, and other storm properties) and its precessing, low inclination (35°) orbit (allowing view of the Tropics and southern portions of Japan and the United States through all hours of the day, so as to observe diurnal cycles of rainfall) (JAXA 2007; Braun 2011).

Before its deactivation, TRMM provided gridded, observed precipitation data over a band around the globe from 35°N to 35°S at a spatial resolution of 0.25° (about 22-kilometers). The first full month of data was January 1998 and the final was March 2015 at temporal resolutions of 3-hour, 10-day, monthly and yearly intervals. The Global Precipitation Measurement (GPM) core observatory satellite was launched by NASA and JAXA on February of 2014 to continue the successful precipitation observation mission. The improved mission specifications will include a satellite constellation capable of providing precipitation maps for studying climate and forecasting extreme weather across the entire planet.

### **3.1.2 Model Processing and Visualization**

The final processing results required all of the datasets to be in a format that could be clipped to the New Mexico study area. CHIRPS, PRISM and TRMM came in geotiff rasters, which were easily clipped using the NM boundary as a mask. The AHPS dataset was clipped by keeping only those projected polygons (Appendix A) that had centroids within the NM boundary mask. The PERSIANN dataset required MatLab (Appendix A) to take the header (Appendix A) and projection for the binary data format and convert it to a raster format useable in ArcGIS. AHPS, CHIRPS, PRISM and TRMM were already in yearly resolutions and once clipped, were ready to be visualized and analyzed. PERSIANN was the only dataset that had to be aggregated from daily temporal divisions into single year resolution.

After clipping all models to the NM border, values were extracted from all cells and a mean precipitation depth was extracted for the entire state. In the case of models that contained null values, the null values were not included when calculating the mean. The pixel count however, was not reduced and the total was still multiplied by the mean depth to obtain the final volume. This yearly mean value was then multiplied by the total surface area of 77,886,134 acres and multiplied by approximately 0.0328 feet per millimeter to determine a volume in acre-feet. The final values were kept as both millimeters of depth and acre-feet per year. The symbology (Appendix A) for the spatial analysis was achieved by determining the highest and lowest values displayed over the temporal study time for all eight precipitation and evapotranspiration models. A multivariable color ramp was developed to provide the widest detection of different values possible, where 0 millimeters (0 inches, 0 acre-feet) was placed at the red end and 1625.6 millimeters (64 inches, 21,086 acre-feet) was placed at the purple end.

### **3.1.3 Model Statistics**

Only the most basic of statistics were generated for phase one in order to get a sense of the differences between each model. A precipitation/evapotranspiration mean, component means, and yearly means for each model and across all years were calculated and compared. A wet year and a dry year in the New Mexico study area was determined based on the highest and lowest available yearly mean values for all models. Individual cell values were also collected together in Excel spreadsheets and histograms were built using percentages of cells that held specific values.

## 3.2 Comparison Results

### 3.2.1 Model Visualization and Spatial Analysis

The distribution of the highest precipitation values around the state fell around the mountainous features for most of the models (Figures 4 to 8). Finer resolutions of around 4 kilometers showed the topography better than the coarser (5 to 25 kilometer) ones did. Yearly variations of precipitation values for all models were large, showing less or more volume around the state in many areas. However, mountain and valley features remained visible in most of the models.

CHIRPS, PRISM and TRMM had well defined regions of topography that remained high in value, even during dry years. Mountains displayed more prominently on the PRISM results with its finer resolution. The coarse resolution of TRMM showed fewer mountain delineations, but the values were still high in the general vicinity. AHPS had a few topographically defined regions in Chaco Canyon (Appendix A) and a couple of the mountain ranges, but there were striated areas of extremely high and low values that interfered with visualization. It was assumed that these patches, which remained from year to year, were radar signal issues or transition from radar rich to radar poor coverage areas. PERSIANN had no discernable topographically defined regions in its results except perhaps in the northeast corner of the state. This model also had striated areas of high and low values, but these displayed as a cross-hatch pattern that persisted from year to year. These were assumed to be a satellite signal error.

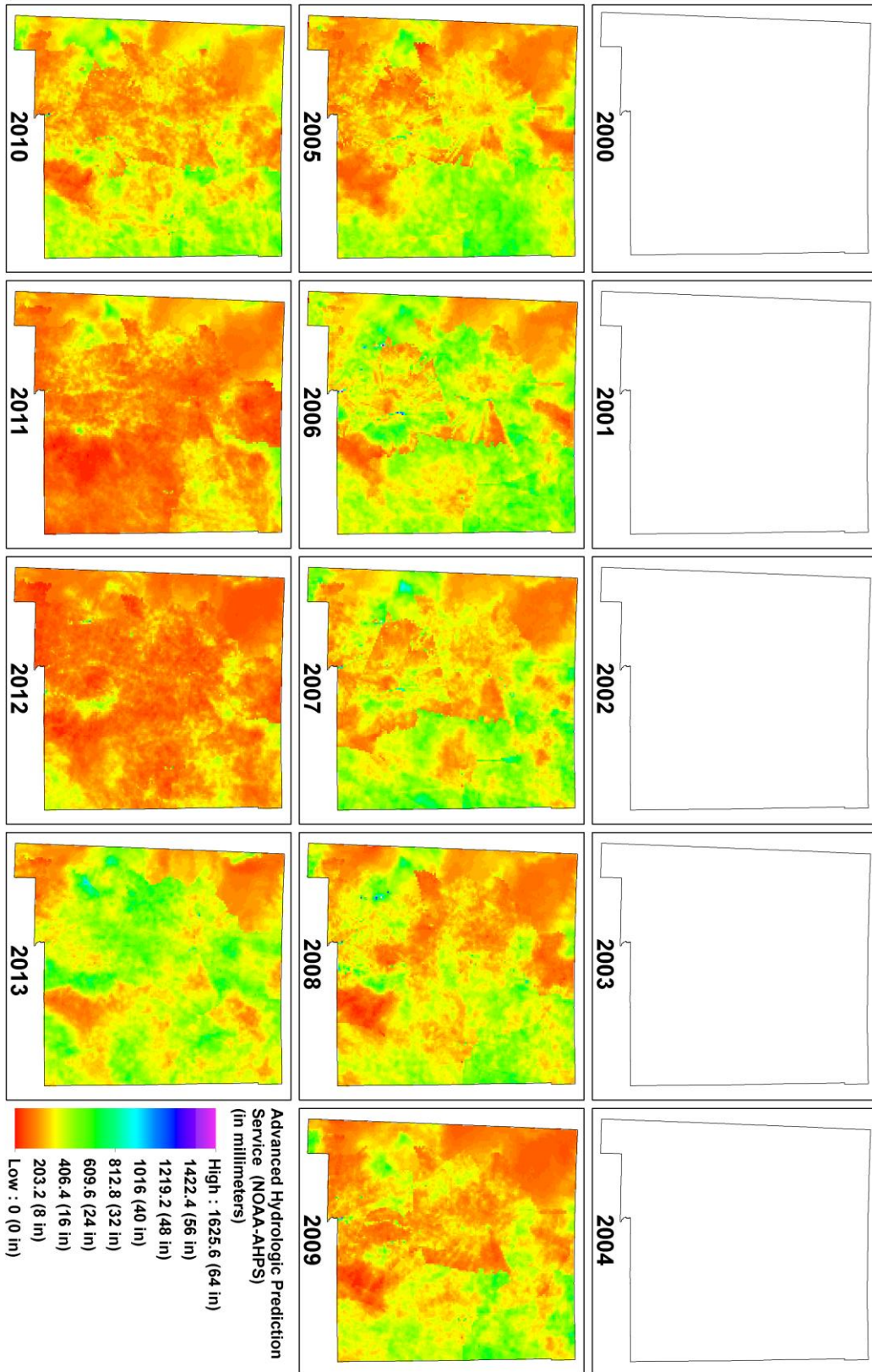


**Figure 4.** AHPS Model Yearly Spatial Results.

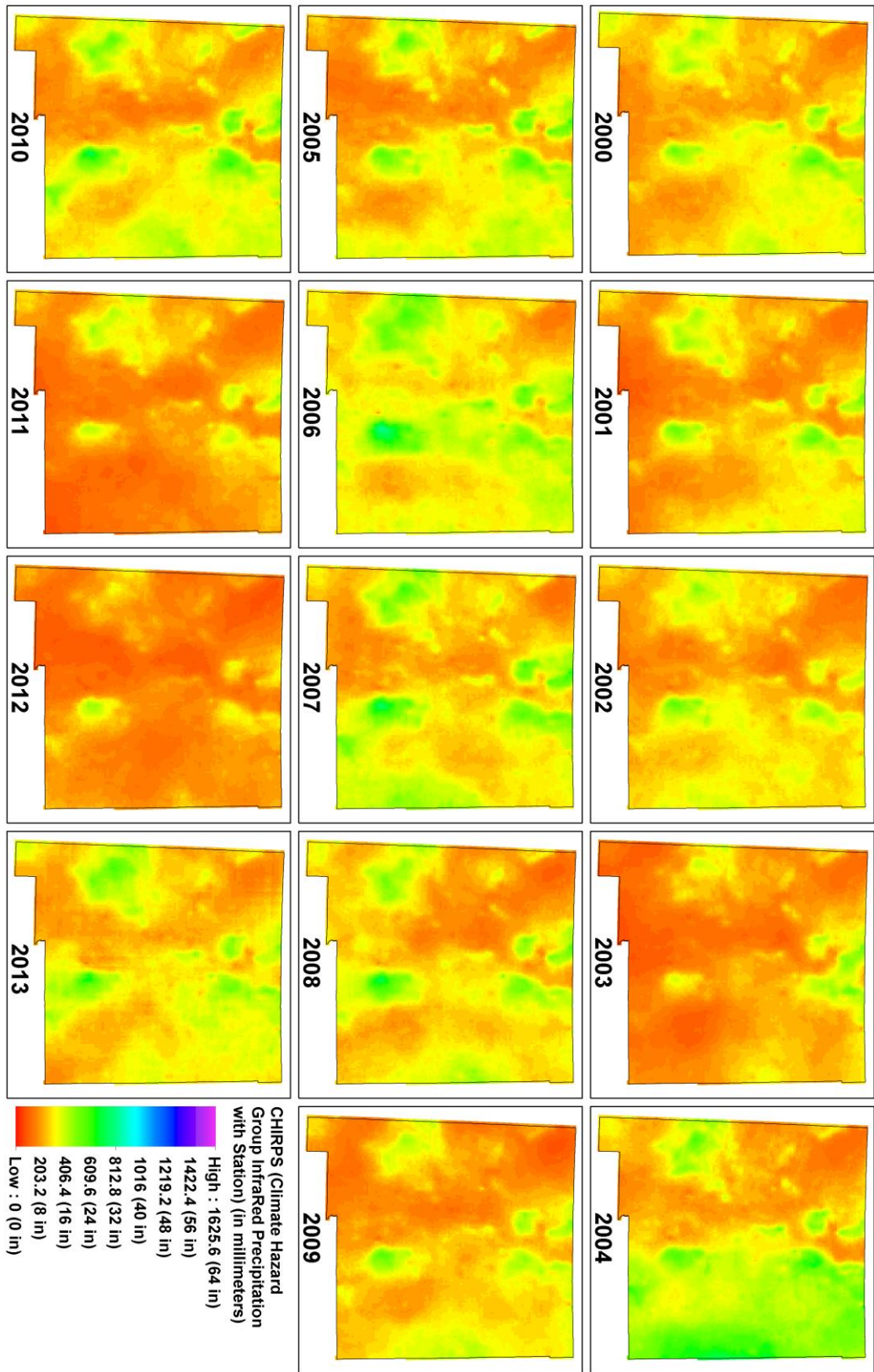


**Figure 5.** CHIRPS Model Yearly Spatial Results.

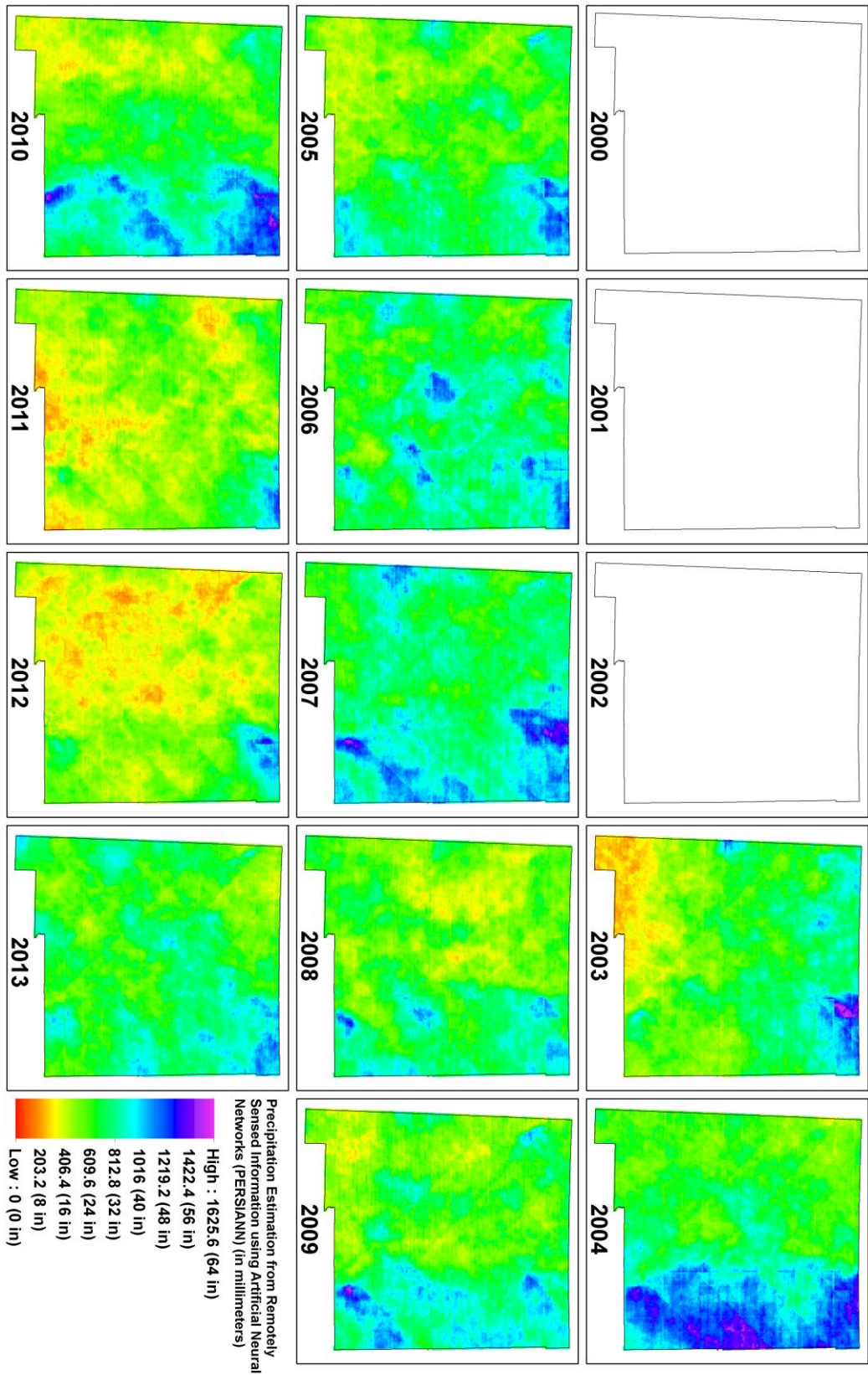


Figure 6. PERSIANN Model Yearly Spatial Results.

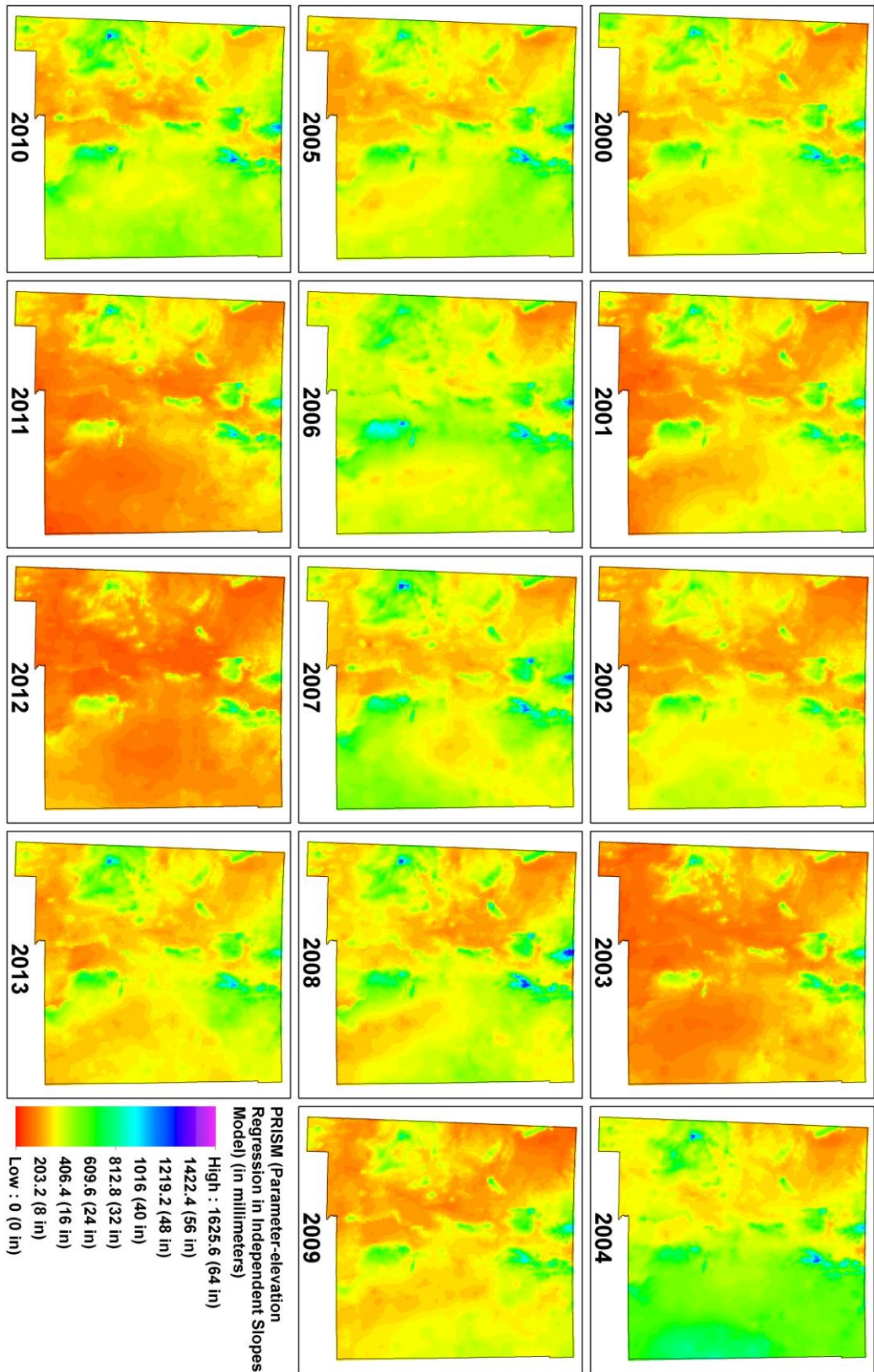
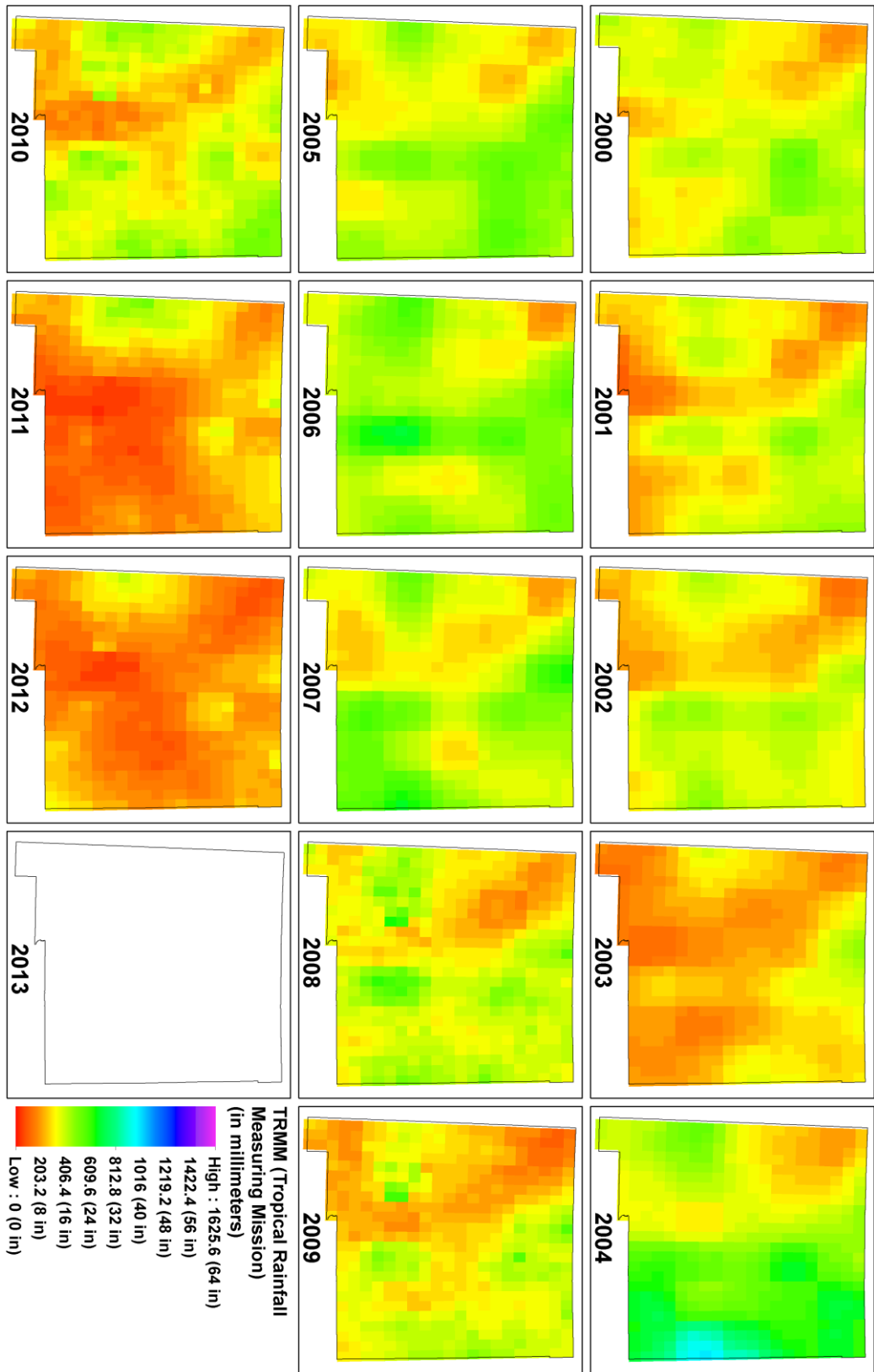


Figure 7. PRISM Model Yearly Spatial Results.



**Figure 8.** TRMM Model Yearly Spatial Results.

### 3.2.2 Statistical Analysis

Each cell or pixel of data represents a value that was converted to a volume of water for the geographic area that the cell or pixel covers during the year. When the cells or pixels are added up for the entire state, the volume represents the total amount of water entering the cell as precipitation. The mean values for each year and the component as a whole pinpointed the model that had the most normalized value amongst the eight. The statistical analyses of the models looked at individual cell or pixel count basic statistics (mean and difference from the component mean) and yearly mean values color coded by the three highest and lowest values for wet and dry year determination (Table 2), a graphic display of all models plotted together (Figure 9) and the cell or pixel percent frequency histogram distributions (Figures 10 and 11) for data symmetry and modal (Appendix A) activity.

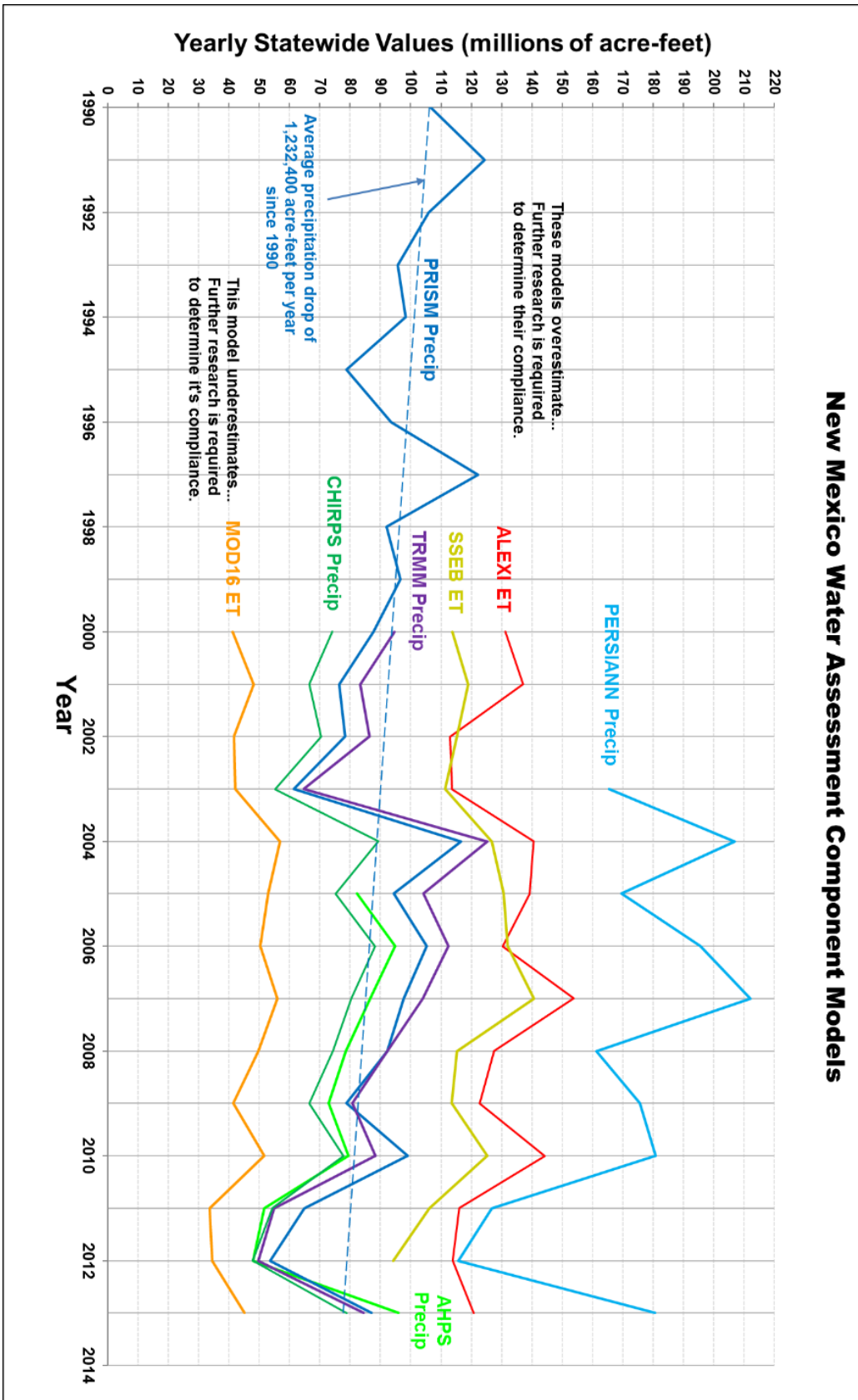
The top section of Table 2 shows that 2007 was the wettest year for three of the models, second wettest for one and third wettest for two. 2004 was considered even wetter than 2007 based on the model yearly means, but AHPS was not functioning at that time, so the wet year was chosen as 2007. The driest year for all models except two was 2012. Model data was extracted for these two years to show the set of extremes within the project for display purposes. The bottom section of Table 2 shows that both precipitation and evapotranspiration component means are nearly equal, indicating that this value is suitable for normalization across models. CHIRPS was 38% lower than the precipitation component mean, AHPS was 29% lower, PRISM was 13% lower and TRMM was 11% lower. PERSIANN was 74% higher than the component mean.

Figure 9 shows that AHPS, CHIRPS, PRISM and TRMM plot relatively close to one another in the center of the graph, while PERSIANN plots extremely high above them. The values of the previous four models also follow nearly the same pattern of highs and lows, falling and rising at nearly the same rate as each other. PERSIANN is far removed from this pattern, but it can still be seen in a few places. Even the evapotranspiration values roughly follow this pattern. A hashed line drawn from the trend shown in the PRISM data indicates that the average precipitation has been dropping by 1,232,400 acre-feet per year since the year 1990.

New Mexico Water Assessment Component Model Comparison									
Evapotranspiration Components				Precipitation Components					
Year	ALEXI	MOD16	SSEB	AHPS	CHIRPS	PERSIANN	PRISM	TRMM	
1990							106.53 (417)		
1991							124.37 (487)		
1992							105.98 (415)		
1993							95.72 (375)		
1994							98.43 (385)		
1995							78.79 (308)		
1996							93.52 (366)		
1997							122.22 (478)		
1998							92.14 (361)		
1999							96.58 (378)		
2000							87.74 (343)		94.63 (370)
2001							76.48 (299)		83.51 (327)
2002							78.50 (307)		86.38 (338)
2003							61.57 (241)		125.36 (491)
2004							206.94 (810)		104.34 (408)
2005							94.50 (370)		112.56 (440)
2006							80.52 (315)		104.04 (407)
2007							161.37 (632)		92.41 (362)
2008							78.79 (308)		80.83 (316)
2009							77.86 (305)		88.37 (346)
2010							126.83 (496)		55.03 (215)
2011							180.70 (707)		49.87 (195)
2012							87.19 (341)		84.52 (331)
2013									
Component Mean	98.00 (383)			99.00 (386)					
Mean (2000-13)	128.93 (505)	46.17 (181)	118.83 (465)	76.76 (300)	71.44 (280)	171.90 (673)	85.32 (334)	87.61 (343)	
Mean Difference	32% Higher	112% Lower	21% Higher	29% Lower	38% Lower	74% Higher	13% Lower	11% Lower	
Cell Count	19217	444943	381760	19752	12599	19583	18087	523	
Null Values	58	10243	0	0	0	0	0	0	
Spatial Res (mi/km)	Continental 2.50 / 4.02	Global 0.52 / 0.84	Continental 0.57 / 0.91	Continental 2.48 / 4.00	Global 3.10 / 4.99	Global 2.51 / 4.04	Continental 2.61 / 4.20	Global 15.77 / 25.38	
Temporal Res	Daily	Monthly, Yearly	Monthly, Yearly	Daily, Monthly, Yearly	Daily, Monthly, Yearly	Daily	Daily, Monthly, Yearly	3 hour, 10 day, Monthly, Yearly	

**Table 2.** Water Assessment Component Model Comparisons.

## New Mexico Water Assessment Component Models



**Figure 9.** Water Assessment Component Models Graphic Display.

The histograms shown in Figures 10 and 11 show that for the wet year the percentage of values are well distributed amongst high and low values. The widths of the curves are all nearly equal, with the exception of the PERSIANN model, indicating that all models except PERSIANN have nearly similar variability amongst them. The amount of offset and location of the peak mimic the percent difference from the component mean and the model mean. All of the models appear to be skewed towards lower values and this would be normal since New Mexico has primarily a steppe environment (Appendix A). The multi-modal CHIRPS, PRISM and TRMM values would indicate that specific areas have an abundance of similar values, such as mountains and valleys. The histograms for the dry year show that AHPS, CHIRPS, PRISM and TRMM have nearly similar distributions with high percentage of low values in the 5 to 7-inch range. Again, PERSIANN differs from the norm displaying a much more varied curve with a high percentage of values in the 14-inch range. Having the models collected together with less variability in the low percentages is what would be expected from a normal model in a dry environment. It is very clear from these histograms that the PERSIANN model is far from accurate in the state of New Mexico.

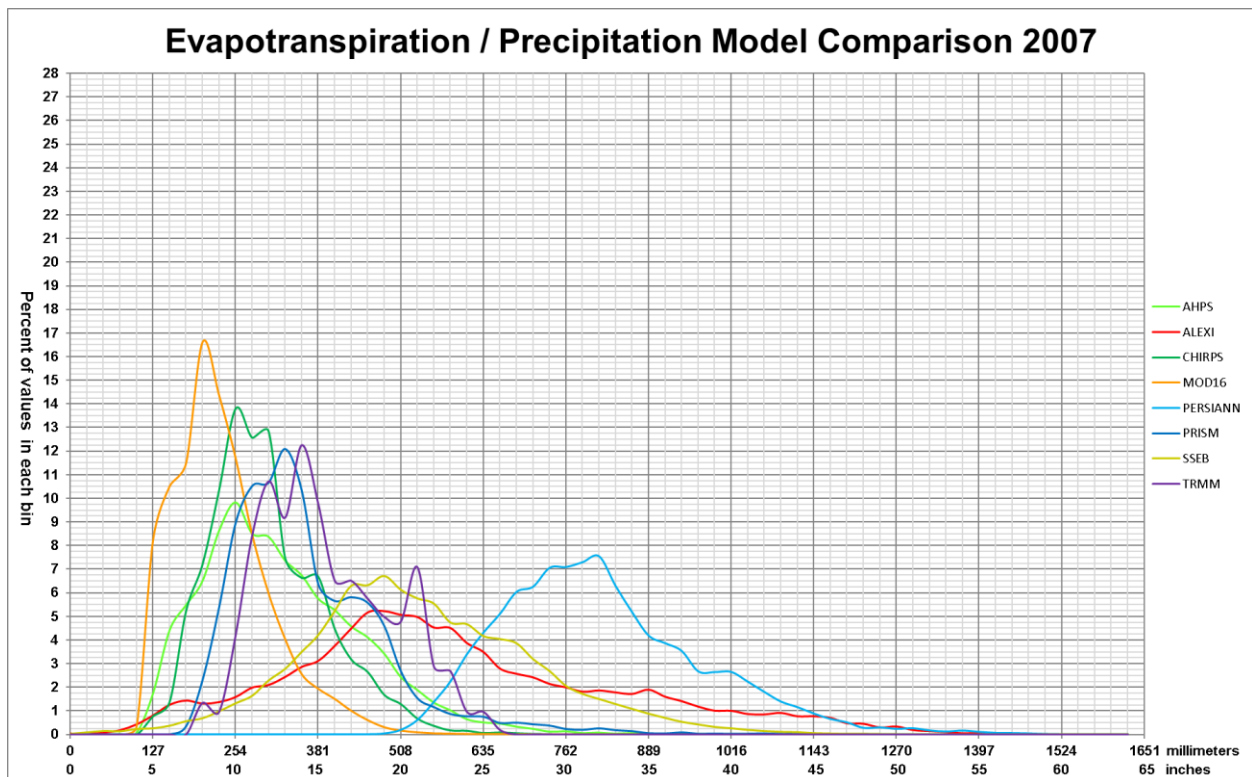


**Figure 10.** 2007 Wet Year Model Histogram Comparison

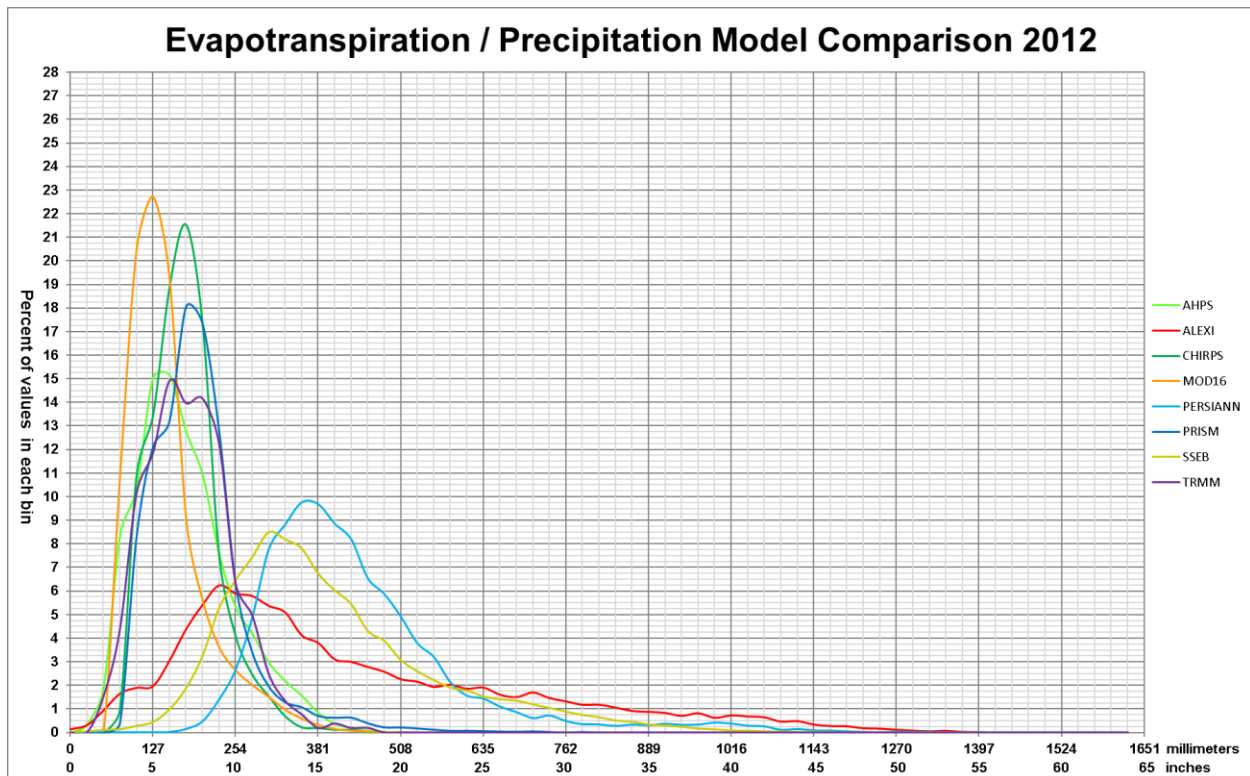


**Figure 11.** 2012 Dry Year Model Histogram Comparison

### 3.2.3 Precipitation Model Advantages and Disadvantages

The end of phase one culminated in several graphic displays and tables of each model’s yearly volume of estimated precipitation in acre feet hitting the ground in New Mexico. Along with these documents, a list of advantages and disadvantages (Table 3) for each model was created to summarize the difficulty of acquisition and processing and the abilities and overall results of each model. At the end of phase one the first preliminary conclusions were made about which models might actually have a chance to proceed to phase three. PERSIANN was easily selected as one that would not and PRISM was the favorite to proceed. This selection would take place after all models were verified using ground station rain gauge values in the next phase.

	<b>Advantages</b>	<b>Disadvantages</b>
<b>AHPS</b>	<ul style="list-style-type: none"> <li>~ Free download</li> <li>~ Values close to component mean</li> <li>~ NM graph near average</li> <li>~ Histogram similar to others</li> <li>~ Precipitation spatial patterns mostly favor mountains</li> </ul>	<ul style="list-style-type: none"> <li>~ Not a raster</li> <li>~ Coarse resolution</li> <li>~ Model uses PRISM starting in 2005</li> <li>~ Discontinuous spatial banding from RADAR not in use on both sides of continental divide</li> </ul>
<b>CHIRPS</b>	<ul style="list-style-type: none"> <li>~ Free download</li> <li>~ Values close to component mean</li> <li>~ NM graph near average</li> <li>~ Histogram similar to others</li> <li>~ Precipitation spatial patterns favor mountains</li> </ul>	<ul style="list-style-type: none"> <li>~ Coarse resolution</li> </ul>
<b>PERSIANN</b>	<ul style="list-style-type: none"> <li>~ Free download</li> </ul>	<ul style="list-style-type: none"> <li>~ Coarse resolution</li> <li>~ Values much higher than component mean</li> <li>~ GOES satellite imagery starts in 2003</li> <li>~ NM graph much higher than average</li> <li>~ Histogram dissimilar to majority</li> <li>~ Poor spatial correlation with any land features</li> <li>~ Hatched striations of discontinuous values</li> <li>~ Extreme precip values during a dry year</li> </ul>
<b>PRISM</b>	<ul style="list-style-type: none"> <li>~ Free download</li> <li>~ Values very close to component mean</li> <li>~ NM graph near average</li> <li>~ Histogram similar to others</li> <li>~ Precipitation spatial patterns favor mountains</li> <li>~ Nearly identical spatial variation to TRMM</li> </ul>	<ul style="list-style-type: none"> <li>~ Coarse resolution (high resolution for a fee)</li> </ul>
<b>TRMM</b>	<ul style="list-style-type: none"> <li>~ Free download</li> <li>~ Values very close to component mean</li> <li>~ NM graph near average</li> <li>~ Histogram similar to others</li> <li>~ Precipitation spatial patterns favor mountains</li> <li>~ Nearly identical spatial variation to PRISM</li> </ul>	<ul style="list-style-type: none"> <li>~ Not raster requires much processing</li> <li>~ Very coarse resolution</li> </ul>

**Table 3.** Precipitation Model Advantages and Disadvantages.

## **4.0 PHASE TWO PROCESS**

### **4.1 Methodology – Verification and Validation**

#### **4.1.1 Field Data Collection**

In situ precipitation measurements for the study come from 60 rain gauges (Table 4) in four counties located in a 75 by 235-mile swath throughout west-central New Mexico (Figure 12). These rain gauges were verified as not having been used to produce any of the precipitation models being tested to prevent any bias on their part. Verification of the model datasets in this phase used 34 rain gauges from the Jornada Experimental Range (ER), 10 from the Sevilleta National Wildlife Refuge (NWR) and 6 extra (from the evapotranspiration verification set) rain gauges from the AmeriFlux Carbon, Water, and Energy Flux Network. The gauges are found in a variety of ecological conditions ranging from lowlands desert shrub and grassland to mountainous juniper and savanna to alpine ponderosa and conifer.

When phase two was started, yearly model rasters had already been processed for spatial analysis and these were used building the model correlations. Data from the thirty-four precipitation gauges at the Jornada ER were already in hand, so the first validation pass was made just using those. The rest of the rain gauges were discovered and collected as phase two progressed.

##### **4.1.1.1. Rain Gauges of the Jornada Experimental Range**

The Jornada ER is located in the northern Chihuahuan Desert, about 25 kilometers northeast of Las Cruces. The range funds and provides data for research focused on desertification, transitions between woody plants, grasslands and human dominated states, water mediation, patch-scale by wind, water, animals, and landscape context (New Mexico State University 1982). As a result, the range maintains a tightly knit collection of rain gauges to help monitor the environmental trends of the enclosed basin area. Four of the stations are located in the San Andres Mountains, east of the flat Jornada del Muerto watershed, and have elevations of over 5000 feet above standard sea-level (ASL). The precipitation measuring units used at each of the sites are Belfort AEPG 600 all-weather precipitation weighing gauges. They have 50.26 square inch basins and are heated to reduce snow occlusion. The monthly measurement data obtained from Jornada covered periods from January 2000 to December 2013 and were aggregated into yearly values.

Agency	ID#	Gauge Name	Est	Term	Latitude	Longitude	Elev	Collection Method		
Jornada	1	Headquarters	1915	On Going	32.61697633	-106.7410545	4324	Weighing Rain Gauge: Belfort AEPG 600, 50.26 sq in		
	2	West Well	1918	On Going	32.60510632	-106.8453266	4334			
	3	Redlake	1918	On Going	32.70897949	-106.8212595	4318			
	4	Ropes Springs	1918	On Going	32.67735007	-106.560303	5659			
	5	South Well	1919	On Going	32.53776242	-106.7462799	4311			
	6	Ragged	1922	On Going	32.56712245	-106.6173871	4724			
	7	Dona Ana Exclosure	1926	On Going	32.48726869	-106.7509264	4350			
	8	Middle Well	1926	On Going	32.6915246	-106.7868515	4311			
	9	Road Tank	1926	On Going	32.67190389	-106.6579253	4633			
	10	Stuart Well	1926	On Going	32.4836811	-106.7333491	4295			
	11	Yucca	1926	On Going	32.57356619	-106.7595593	4331			
	12	Aristida	1927	On Going	32.66490203	-106.8408628	4367			
	13	Brown Tank	1927	On Going	32.61365894	-106.6737737	4452			
	14	New Well	1927	On Going	32.71427181	-106.6257244	4879			
	15	Rabbit	1927	On Going	32.60871378	-106.7969845	4347			
	16	Sandhill	1927	On Going	32.70507016	-106.713586	4518			
	18	Co-op Well	1937	On Going	32.56904643	-106.8116826	4364			
	19	Ash Canyon	1937	On Going	32.61806982	-106.5422121	5709			
	20	Mesquite	1937	On Going	32.64855844	-106.7836536	4331			
	21	Taylor Well	1937	On Going	32.56275925	-106.692389	4370			
	22	Antelope	1938	On Going	32.71961549	-106.7770831	4373			
	23	Parker Tank	1942	On Going	32.64052029	-106.6214089	4734			
	24	Exclosure A	1959	On Going	32.56875143	-106.74425	4331			
	25	Exclosure B	1959	On Going	32.57082033	-106.8013746	4344			
	26	Northeast Exclosure	1959	On Going	32.66797476	-106.7525734	4318			
	29	Saint Nicholas	1963	On Going	32.57995527	-106.5280085	6125			
	30	Pasture 2	1965	2012	32.6175687	-106.8693788	4357			
	31	Goat Mountain	1967	On Going	32.55773871	-106.4897895	6509			
	34	IBP	1970	2012	32.58655494	-106.843592	4344			
	35	Turney	1997	2014	32.69192055	-106.7069528	4478			
	36	Permanent Exclosure 1	1997	2012	32.64692517	-106.86953	4367			
	37	Permanent Exclosure 6	1997	2012	32.69569669	-106.8699894	4383			
	38	Cross Tank	1997	2012	32.60184472	-106.6370828	4583			
	39	Wooton	1997	2014	32.65047588	-106.6835347	4534			
	Sevilleta	1	Headquarters	1989	On Going	34.355984	-106.885264		4724	Tipping-Bucket Rain Gauge, HOBO RG3-M 15.4 cm diam
		40	Deep Well	1988	On Going	34.35922	-106.691116		5249	
		41	South Gate	1989	On Going	34.35922	-106.795439		4970	
		42	Cerro Montosa	1989	On Going	34.368477	-106.535497		6378	
		43	Watersheds	1989	On Going	34.368477	-107.037407		5735	
44		Rio Salado	1989	On Going	34.295956	-106.926649	4872			
45		Bronco Well	1989	On Going	34.405577	-106.934042	5000			
48		Blue Springs	1999	On Going	34.414706	-106.523398	5886			
49		Five Points	1999	On Going	34.334952	-106.729265	5285			
50		Blue Grama	2001	On Going	34.334852	-106.632006	5476			
AmeriFlux		Mpj	Mountainair-Pinon/Juniper	2008	2010	34.4384	-106.2377	7014	Tipping-Bucket Rain Gauge filling gaps with PRISM data	
	Seg	Sevilleta-Desert Grassland	2007	2010	34.3623	-106.7019	5322			
	Ses	Sevilleta-Desert Shrubland	2007	2010	34.3349	-106.7442	5226			
	Vcm	Valles Caldera-Mixed Conifer	2007	2010	35.8884	-106.5321	9852			
	Vcp	Valles Caldera-Ponderosa	2007	2008	35.8624	-106.5974	8340			
	Wjs	Willard-Juniper Savanna	2008	2008	34.4255	-105.8615	6319			

**Table 4.** List of Rain Gauges Used for Validation and Verification of Precipitation Products (Coordinates in GCS-WGS84).

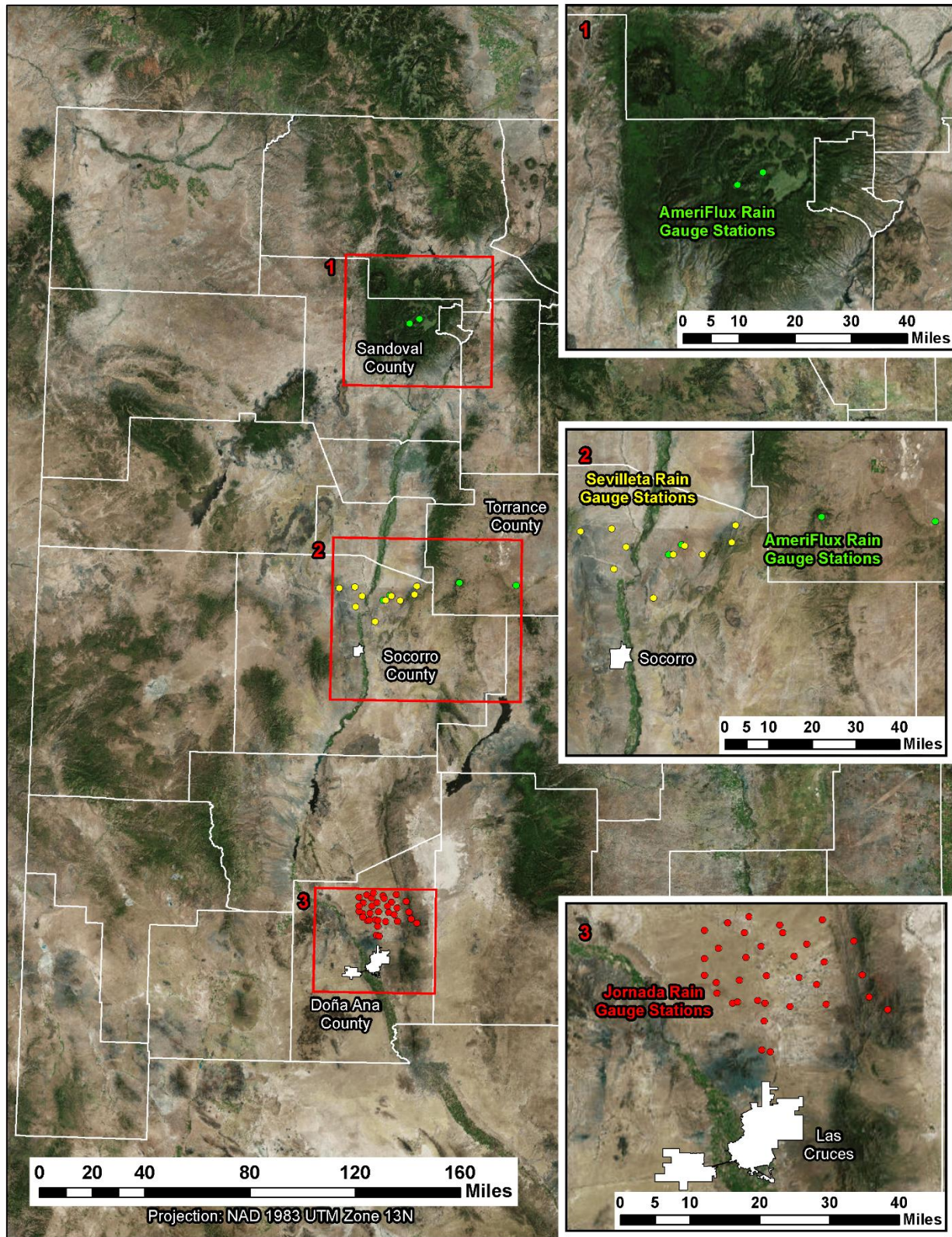


**Figure 12.** Location of Rain Gauges for Validation and Verification of Precipitation Products

#### **4.1.1.2. Rain Gauges of the Sevilleta National Wildlife Refuge**

The primary study site of the Sevilleta NWR is located in central New Mexico, about 32 kilometers north of Socorro. The experimental range funds and provides data for research focused on mechanisms and consequences of climate change on desert grassland, shrubland, woodland, forest and riparian habitats, widespread tree mortality from chronic drought, large fires or insect outbreaks (University of New Mexico, 1994). This range also maintains a collection of rain gauges to help monitor the environmental trends of the study area. Six of the stations are located in the high plains east and west of the Rio Grande, and have elevations of over 5000 feet ASL. The precipitation measuring units used at each of the sites are HOBO RG3 tipping bucket precipitation rain gauge loggers. They have 28.9 square inch basins to collect precipitation. The monthly measurement data obtained from Sevilleta covered periods from January 2000 to December 2013 and were aggregated into yearly values.

#### **4.1.1.3. Rain Gauges of the AmeriFlux Energy Flux Network**

The AmeriFlux Energy Flux Network coordinates regional and global analyses from micrometeorological tower sites that measure exchanges of CO<sub>2</sub>, water vapor, and energy between terrestrial ecosystems and the atmosphere. The FLUXNET database contains information about 650 tower sites that provide long-term and continuous data for land cover, climate, plants and soil; atmospheric flux data measured at each site; and remote sensing products for evaporation, albedo and energy absorption (NASA-Oak Ridge National Laboratory 2014). All AmeriFlux sites are over 5000 feet ASL with three in mountainous regions over 7000 ASL feet. The mountainous sites are populated by piñon/juniper, mixed conifer, and ponderosa pine foliage. All rain gauges are of the tipping bucket variety of an unspecified type. The monthly measurement data obtained from the AmeriFlux sites covered periods from January 2007 to December 2010 and were aggregated into yearly values.

#### 4.1.2 Model Data Extraction

Data was extracted from each of the yearly model layers by using the ArcGIS Extract Multi Values to Points tool on a blank point shapefile (Appendix A) holding the locations of each station. This tool samples each individual input raster or polygon features, adding a field for each in the point shapefile, and extracts and writes the values in the newly added field. Once all values for all months at each station are written, these can be extracted as comma delimited text (Appendix A) files and imported into an Excel spreadsheet for analysis. These values can then be plotted against the dates to obtain precipitation changes over time or differences over time, or against one another in a correlation scatter plot to obtain an R-squared value (Appendix A).

To obtain the root mean square error (RMSE), the station values are listed in a set of rows and the model values at the station locations are listed in rows below them in Microsoft Excel. A set of rows are set up below the station and model values that calculates the difference between the model and station by subtracting the station values from the model values. A sum of the squared residuals is calculated by summing the square (SUMSQ; Excel Function) of each station-model difference pair. After the number of station-model difference pairs is counted (Total cells – COUNTBLANK; Excel Function), the RMSE is calculated by taking the square root of the division of the sum of the squared residuals by the number of station-model difference pairs.

#### 4.1.3 Model Comparison

While phase one was used to explore the data and determine their viability, phase two was used to determine whether the data predicted what was happening accurately. The biggest problem with verification was that there was no sure way of determining exactly what was happening across the entire state. The most feasible method for determining model accuracy is to take field measurements at specific points and choose the model that has the closest values.

The models in phase two are compared through correlation graphs and quantifiable statistical values. R-squared values describe the precision of two variables. The tighter the grouping of variable points and the closer the slope of the trend line to the 1:1 correlation line, the closer the points are to being similar and the higher the R-squared value. The RMSE describes the accuracy of two variables and the ability of one to variable to match another. Squaring the difference magnifies the amount of error and removes negative results. The

correlation graphs show each model as a cloud of colored station-model pairs along with a trend line to indicate the model's overall correlation with the ground data.

#### **4.2 Model Comparison Results**

Of the yearly precipitation comparisons of Jornada ER stations and precipitation models (Figure 13), the PRISM model had the best precision and accuracy with an R-squared value of 0.76 and a RMSE of  $\pm 43.63$  millimeters. AHPS had the worst precision with an R-squared value of 0.37, with a RMSE of  $\pm 60.31$  millimeters. PERSIANN had the worst accuracy with a RMSE of  $\pm 279.07$  millimeters, with an R-squared of 0.56. This was the last bit of proof required to eliminate all other models and continue the project forward with the PRISM model.

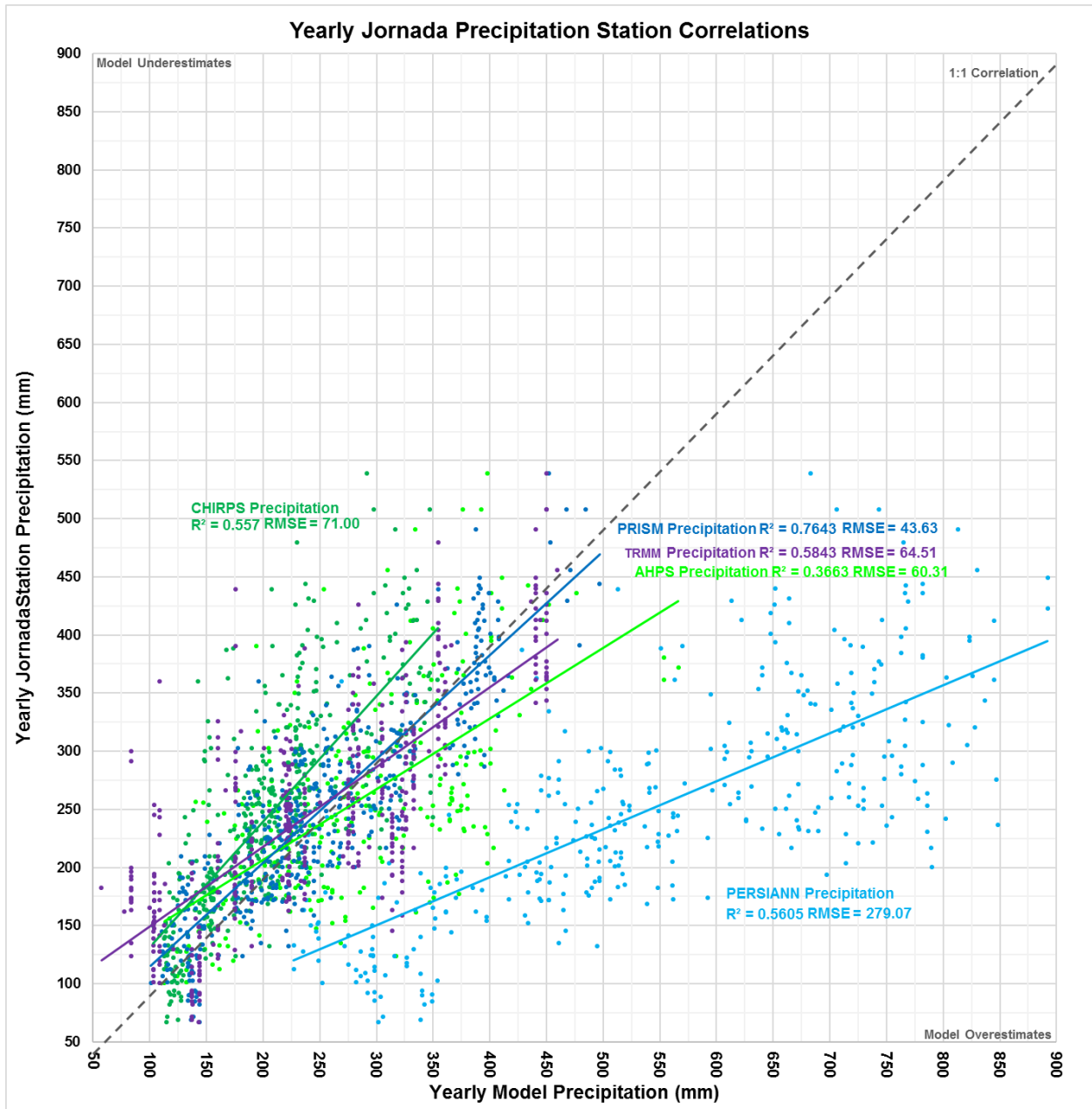


**Figure 13.** Correlation Between Precipitation Models and Jornada ER Rain Gauges.

## **5.0 PHASE THREE PROCESS**

### **5.1 Methodology – Quality Control**

#### **5.1.1 PRISM High Resolution Model Acquisition**

The proposal states that the chosen precipitation products would be fine-tuned and quality controlled by making adjustments to the chosen component model and validate results to the greatest degree possible to predict component values as precisely and accurately as possible for the unique environment of New Mexico. The PRISM dataset used in the original comparisons was a monthly, 4-kilometer resolution dataset that had been aggregated into annual values. The PRISM Climate Group at OSU also has an 800-meter resolution version that is distributed in monthly and daily increments. To satisfy the proposal, this dataset was purchased for the New Mexico Statewide Water Assessment.

#### **5.1.2 Verification of the PRISM M2/D1 High Resolution Model**

To perform the correlations, the pixel values at the location of each field placement were extracted from each model for each month using the Extract Multi Values to Points tool as had been done in phase two, but the interpolation option was set to bilinear to take pixel variation around the field placement into account. This sort of interpolation takes the four nearest pixel centroids to the field placement and applies a distance weighted average to the values to determine the value at the location. Scatter plot correlation graphs and root mean square errors were calculated using the full fifty rain gauge stations instead of the original thirty-four. Verification and validation measurements during this phase were also expanded from yearly resolution to monthly to provide more data points for correlation. These were available over the project period from 2000 to 2013 with 7382 field value measurements to compare against model values.

Obtaining the higher spatial resolution data improved a particular model value variability issue that was observed with coarse resolution model data. This issue affected the final correlations negatively. Since the average distance between Jornada stations was about four kilometers, several stations having differences in measured values had the same model values because they resided in the same model pixel. This was especially true of the TRMM analysis and the graphed values took on a stair-stepped shape with no variation on the X-axis. Even though the 4-kilometer resolution models did not have the stair-stepping, the variation on the X-axis could be low enough to affect the precision ( $R^2$ ) of the model.

The new 800-meter PRISM data (hereon labeled as 800m PRISM M2/D1 for monthly version 2 and daily version 1) eliminated the model value variability issue and also had the added bonus of being trained using NEXRAD Doppler radar observed rain measurements. This further improved the correlations against the Jornada ER ground data. When the 800m PRISM M2/D1 data was first obtained and correlations between it and the Jornada ER ground data were made, it was discovered that the daily PRISM (D1) data aggregated into monthly values did not match the monthly PRISM (M2) data that were sent (Figures 14 to 16). This was because the training from the NEXRAD Doppler radar data was only applied to the daily PRISM data for better real-time estimations and not to the monthly data. Several attempts were performed to determine which dataset (800m PRISM aggregated D1 or the 800m PRISM M2) provided the best correlation and statistics with the measured station data.

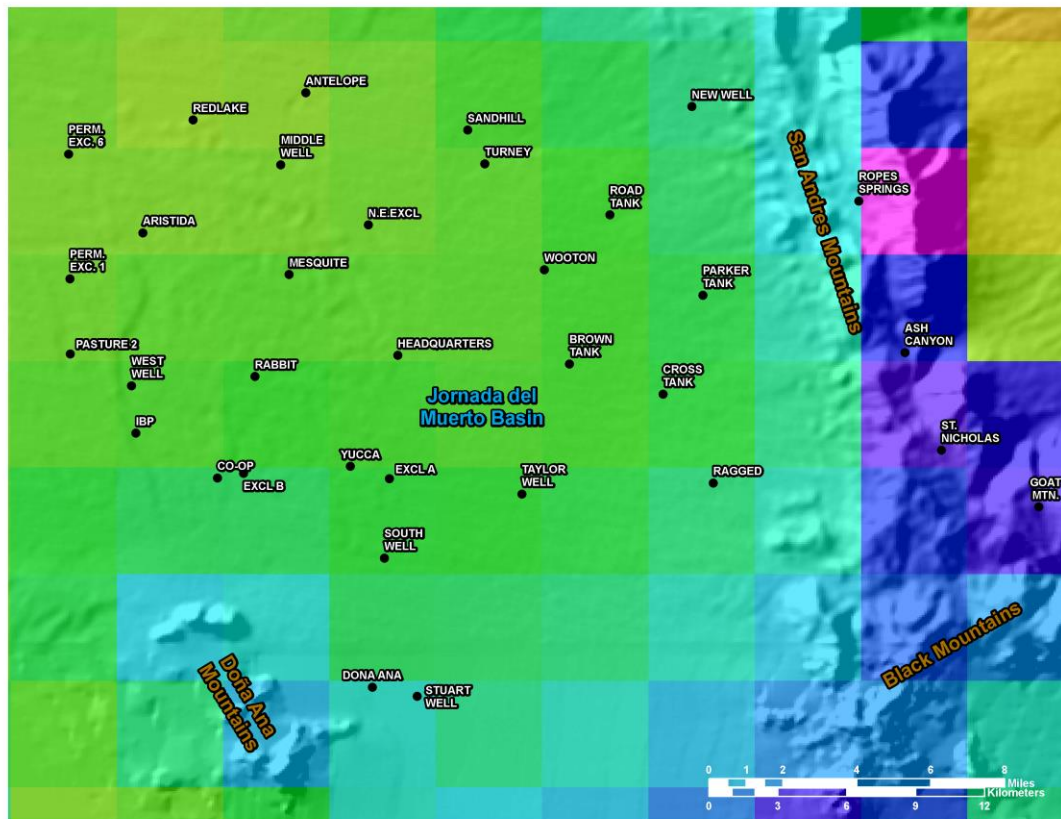


**Figure 14.** 4-kilometer PRISM M2 Precipitation Data at Jornada ER, Aggregated for Year 2008.

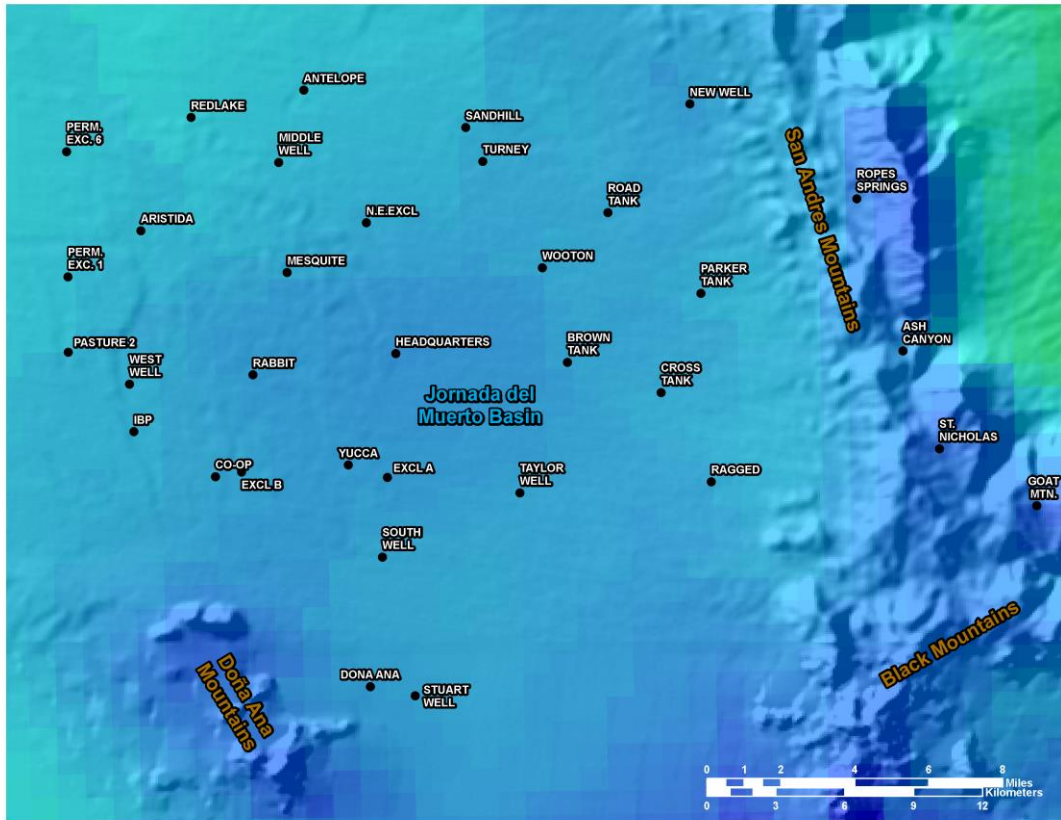


**Figure 15.** 800-meter PRISM M2 Precipitation Data at Jornada ER for July 2008.

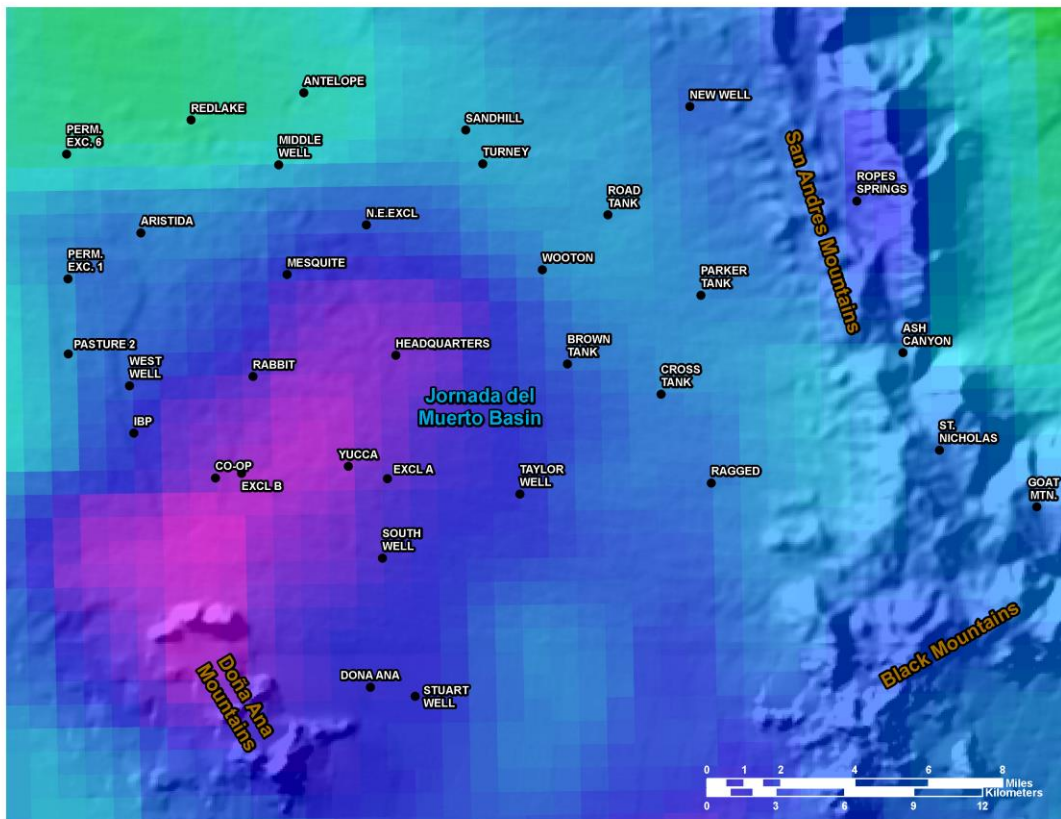


**Figure 16.** 800-meter PRISM D1 Precipitation Data at Jornada ER, Aggregated for July 2008.

These spatial distributions show that the radar enhanced D1 data captures the variations in actual rainfall that the M2 data does not. Results of the aggregated D1 data versus the M2 data showed that small scale variations were present in the aggregated D1 data and not in the M2 data, because the training from the Doppler data added chaotic variation to the D1 data. This chaos has the effect of making the smooth climatologically interpolated M2 data respond more naturally, but it also added more variability to the model, decreasing the precision.

The size of the 800-meter pixels in the new data also provides a wider variation of values between tight groups of rain gauges that the 4-kilometer data might not capture as well. Higher variation from improved resolution and actual radar measurements was expected to provide improved accuracy between the model and the station, but the station correlations (Figures 17 and 18) disagreed. The M2 data without radar measurements had an R-squared value of 0.7716 with a RMSE of 13.37, while the aggregated D1 data had an R-squared value of 0.7660 with a RMSE of 13.98.

The D1 data is enhanced on a pixel-by-pixel basis using Doppler radar that is only available east of the Continental Divide, leaving the portion of New Mexico west of the Divide to use only the unaltered climatologically aided interpolation. This process is not performed on the M2 data, leading to discrepancies between aggregated D1 grid values and M2 grid values. As of July 2015, the data were revised (M3/D2) by the PRISM Climate Group to force the monthly gridded values to equal the daily aggregated values at the end of the month. These data were requested and sent without charge and the verification process was started over again.

### **5.1.3 Verification of the PRISM M3/D2 High Resolution Model Revision**

The 800-meter, monthly PRISM M3 values were compared to the previous M2 and aggregated D1 datasets and to the full set of rain gauges for each month between January 2000 and December 2013 as they had been previously. Spatial distribution maps and graphs of monthly accumulation and station correlations were created to determine differences. The newly revised M3/D2 dataset description claims that in the mountainous terrain areas in the western United States (Rockies westward), the D2 daily grid values are forced to sum to the M3 monthly grid values, because interpolation of longer time-step data better captures persistent orographic precipitation patterns than daily interpolation (University of Oregon 2015). Reverse forcing is performed east of the Continental Divide, where the M3 monthly grid values are forced to equal the aggregated D2 daily grid values, similar to the aggregated product verified in the last section.

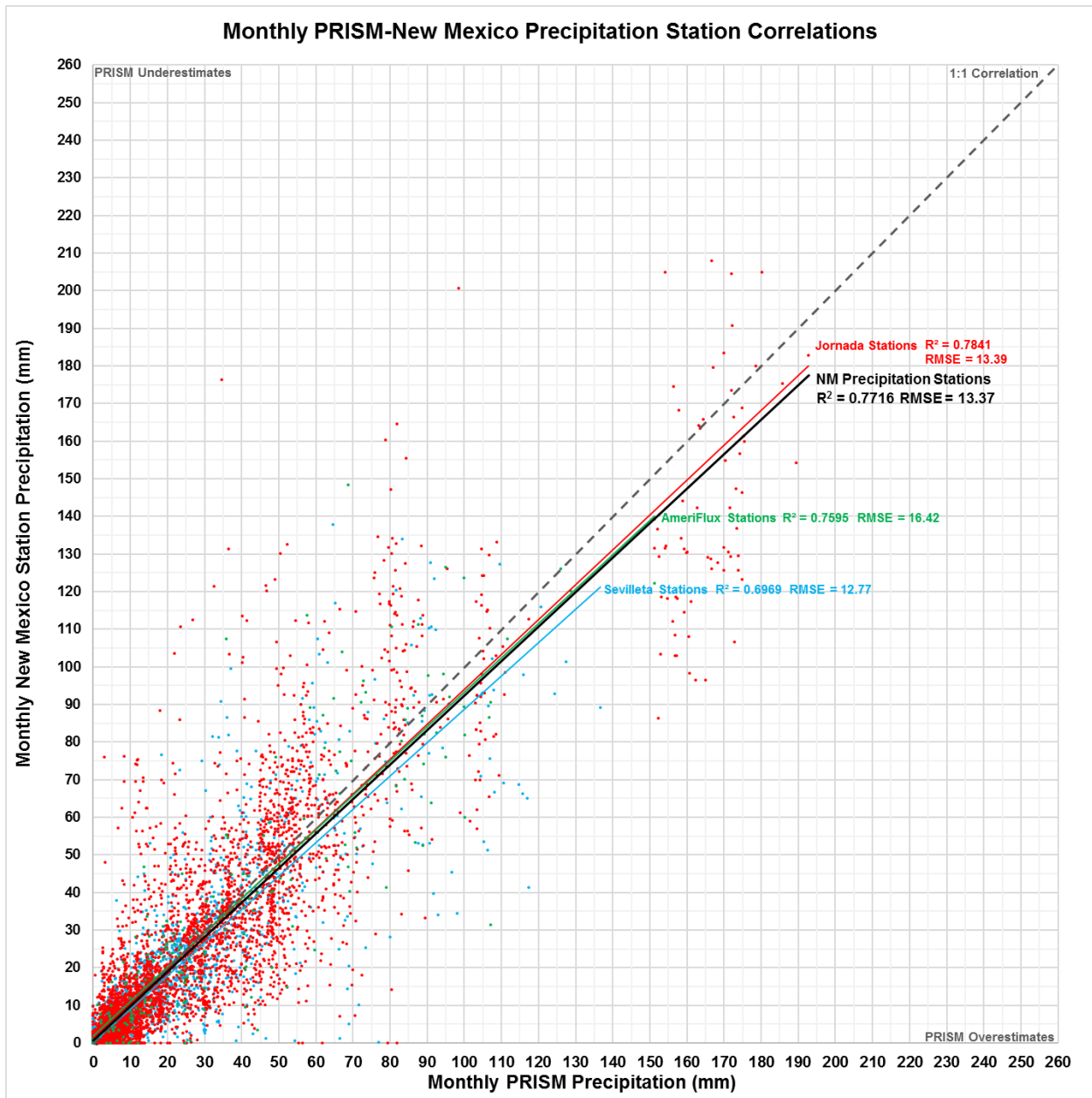
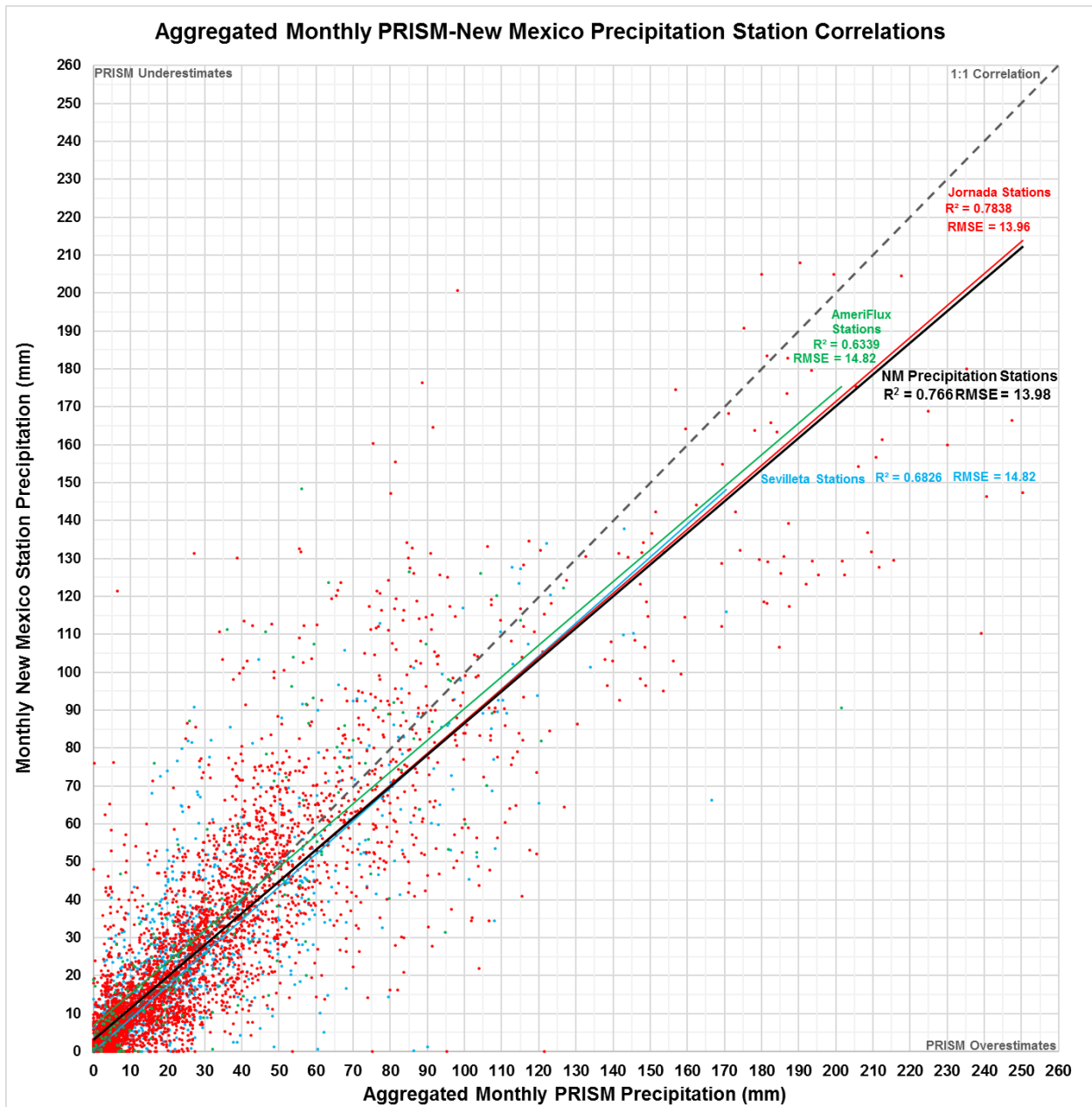


Figure 17. 800-meter PRISM M2 Correlation with New Mexico Precipitation Stations.



**Figure 18.** 800-meter PRISM Monthly D1 Aggregation Correlation with NM Precipitation Stations

## 5.2 PRISM M3/D2 High Resolution Revision Results and Conclusion

As claimed, the aggregated D2 data values do equal the monthly values and thus, the final set of calculations are only required for the monthly data. The results of the new M3 revised data were an overall improvement over all previous PRISM data yielding an R-squared value of 0.7908 with a RMSE of 13.26. This improvement was most likely due to an improvement in the CAI interpolation method within New Mexico’s border, since there was an improvement from M2 to M3 that would not have come from forcing to shorter time-step data.

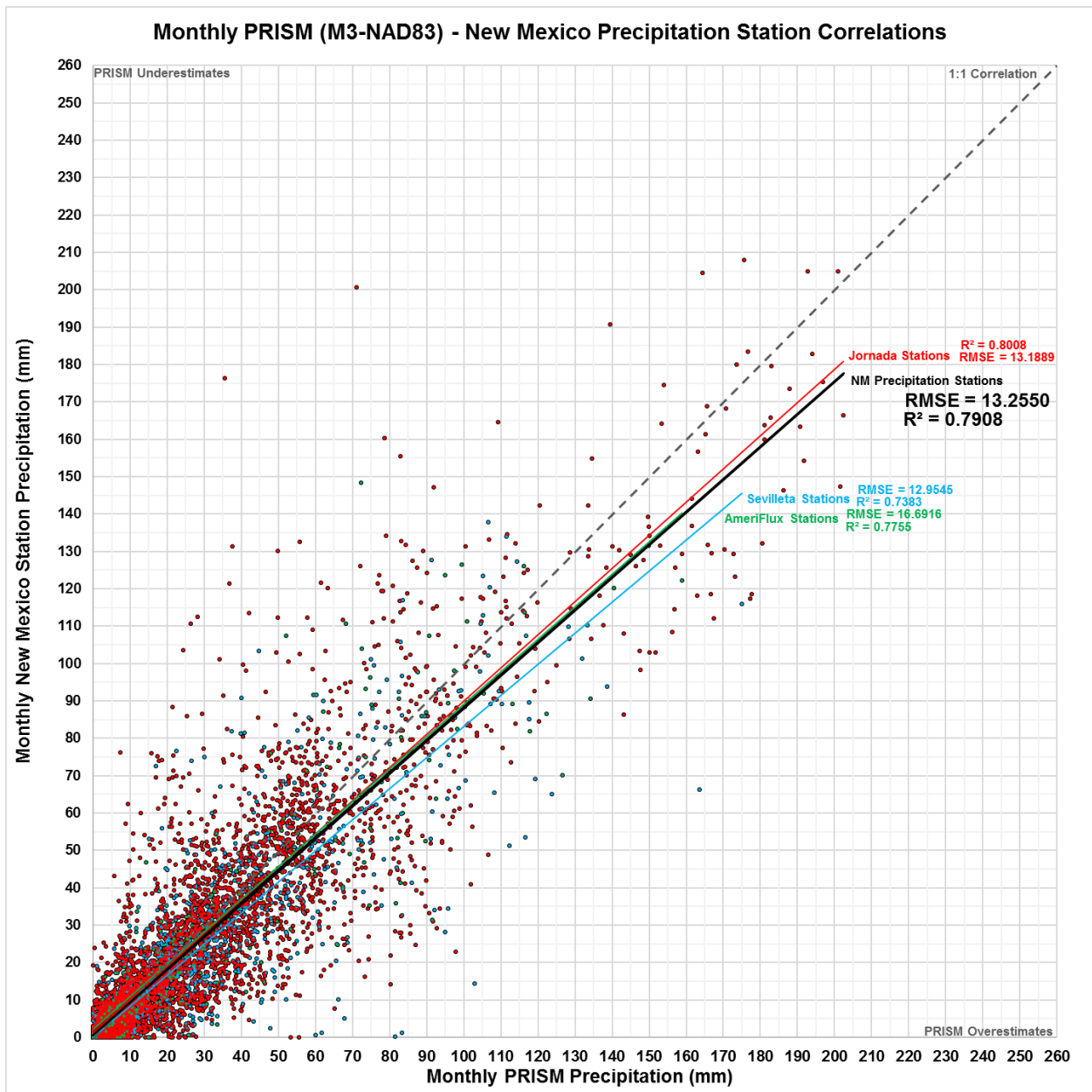


Figure 19. 800-m PRISM M3 Correlation with NM Precipitation Stations

## 6.0 PHASE FOUR PROCESS

### 6.1 Continuing Forward with Precipitation Component Data Dissemination

With the verification, validation and quality control of the monthly 800-meter PRISM M3 gridded precipitation product, the set of 360 rasters (30 years × 12 months) has been clipped to the New Mexico Headwaters mask to provide monthly precipitation estimates for subbasin hydrologic units (HUC-8), counties and water planning regions (Appendix A). These monthly values will then be inserted into a Dynamic Statewide Water Budget estimator (Figure 20) in an attempt to determine the best way to incorporate precipitation into the model. Now that the model has been acquired and processed, a set of scripts (Appendix A) will have to be produced that will constantly process newly acquired PRISM data and make them available for the estimator, as well as for server based displays that can produce graphs, tables and statistics for the public.

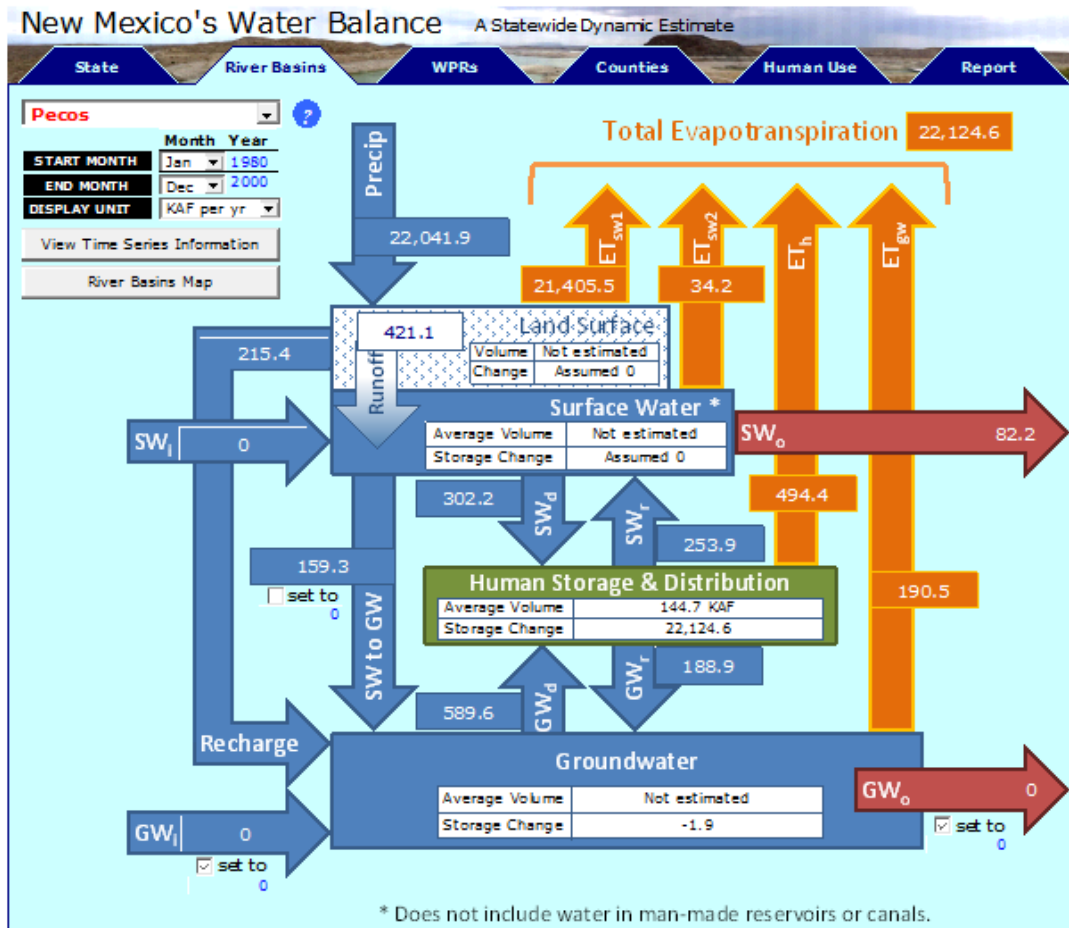


Figure 20. Dynamic Statewide Water Budget Estimator

## 7.0 REFERENCES

- Austin P. 1987. "Relation between measured radar reflectivity and surface rainfall." *Monthly Weather Review*. 115 (5): 1053-70.
- Braun, S. 2011. *Tropical Rainfall Measuring Mission: Senior Review Proposal*. Washington, D.C.: National Aeronautics and Space Administration.
- Daly, C., R. Neilson, and D. Phillips. 1993. "A statistical-topographic model for mapping climatological precipitation over mountainous terrain." *Journal of Applied Meteorology* 30: 140-158.
- Daly, C., G. Taylor, and W. Gibson. 1997. "The PRISM approach to mapping precipitation and temperature." *10th AMS Conference on Applied Climatology*. Reno, NV. 10-12.
- Daly C. 2013. "The PRISM climate and weather system: An introduction." *Crop Insurance Today* 46 (3): 4-8.
- Environmental Modeling Center, National Center for Environmental Prediction, National Weather Service, NOAA. 2011. "NCEP Climate Forecast System Version 2 (CFSv2) 6-hourly Products. Research Data Archived at the National Center for Atmospheric Research, Computation and Information Systems Laboratory." <http://rda.ucar.edu/datasets/ds094.0/> (Accessed June 30, 2015).
- Fread, D, R. Shedd, G. Smith, R. Farnsworth, C. Hoffeditz, L. Wenzel, S. Wiele, J. Smith, and G. Day. 1995. "Modernization in the National Weather Service river and flood program." *Weather and Forecasting*. 10 (3): 477-484.
- Funk, C., J. Michaelsen, J. Verdin, G. Artan, G. Husak, G. Senay, H. Gadain, and T. Magadzire. 2003. "The collaborative historical African rainfall model—description and evaluation" *International Journal of Climatology*. 23: 47–66.
- Funk, C., and J. Michaelsen. 2004. "A simplified diagnostic model of orographic rainfall for enhancing satellite-based rainfall estimates in data poor regions." *Journal of Applied Meteorology*. 43: 1366–1378.
- Funk, C., G. Senay, A. Asfaw, J. Verdin, J. Rowland, J. Michaelsen, G. Eilerts, D. Korecha, and R. Choularton. 2005. *Recent drought tendencies in Ethiopia and equatorial-subtropical eastern Africa: Famine Early Warning System Network Special Report*. Washington, D.C. U.S. Agency for International Development.
- Funk, C., G. Husak, J. Michaelsen, T. Love, and D. Pedreros. 2007. "Third generation rainfall climatologies—Satellite rainfall and topography provide a basis for smart interpolation." In *Crop and Rangeland Monitoring Workshop, 2<sup>nd</sup> Edition Extended Abstract*. Nairobi, Kenya.
- Funk, C., and J. Verdin. 2010. "Real-time decision support systems—The famine early warning system network." In *Satellite Rainfall Applications for Surface Hydrology*, 2010 edition, 295–320. Springer, Netherlands, Springer.
- Funk, C., J. Michaelsen, M. Marshall. 2012. "Mapping recent decadal climate variations in precipitation and temperature across Eastern Africa and the Sahel." In *Remote Sensing of Drought—Innovative Monitoring Approaches*, Chapter 14. Milton Park, Abingdon. Taylor and Francis.

- Funk, C., P. Peterson, M. Landsfeld, D. Pedreros, J. Verdin, J. Rowland, B. Romero, G. Husak, J. Michaelsen, and A. Verdin. 2014. *A quasi-global precipitation time series for drought monitoring*. Data Series 832. Reston, VA. United States Geological Survey.
- Huffman, G., D. Bolvin, E. Nelkin, D. Wolff, R. Adler, G. Gu, and E. Stocker. 2007. "The TRMM multisatellite precipitation analysis (TMPA)—Quasi-global, multiyear, combined-sensor precipitation estimates at fine scales." *Journal of Hydrometeorology*. 8 (1): 38–55.
- Huffman, G., R. Adler, D. Bolvin, and E. Nelkin. 2011. "The TRMM multi-satellite precipitation analysis (TMPA)." In *Mekonnen Gebremichael, Faisal Hossain, Satellite rainfall applications for surface hydrology*. 3–22. Netherlands, Springer.
- Husak, G., J. Michaelsen, and C. Funk. 2007. "Use of the gamma distribution to represent monthly rainfall in Africa for drought monitoring applications." *International Journal of Climatology*. 27 (7): 935–944.
- Hsu, K., X. Gao, S. Sorooshian, and H. Gupta. 1997. "Precipitation estimation from remotely sensed information using artificial neural networks." *Journal of Applied Meteorology*. 36 (9): 1176–1190.
- Hsu, K., H.V. Gupta, X. Gao, and S. Sorooshian. 1999. "A neural network for estimating physical variables from multi-channel remotely sensed imagery: application to rainfall estimation." *Water Resources Research*. 35: 1605-1618.
- Janowiak, J., R. Joyce, and Y. Yarosh. 2001. "A real-time global half-hourly pixel-resolution infrared dataset and its applications." *Bulletin of the American Meteorological Society*. 82 (2): 205–217.
- Japan Aerospace Exploration Agency. 2007. "What's TRMM? Basic Information about the Tropical Rainfall Measuring Mission (TRMM) satellite, including overview of satellite and sensors." [http://www.eorc.jaxa.jp/TRMM/about/top\\_e.html](http://www.eorc.jaxa.jp/TRMM/about/top_e.html) (Accessed June 30, 2016).
- Knapp, K., S. Ansari, L. Bain, M. Bourassa, M. Dickinson, C. Funk, C. Helms, C. Hennon, C. Holmes, G. Huffman, J. Kossin, H. Lee, A. Loew, and G. Magnusdottir. 2011. "Globally gridded satellite (GriSat) observations for climate studies." *Bulletin of the American Meteorological Society*. 92 (7): 893–907.
- Kummerow, C., J. Simpson, O. Thiele, W. Barnes, A. T. C. Chang, E. Stocker, R. F. Adler, A. Hou, R. Kakar, and F. Wentz. 2000. "The status of the Tropical Rainfall Measuring Mission (TRMM) after two years in orbit." *Journal of Applied Meteorology* 39: 1965-1982.
- Lawrence B., M. Shebsovich, M. Glaudemans, and P. Tilles. 2003. "Enhancing precipitation estimation capabilities at National Weather Service field offices using multi-sensor precipitation data mosaics." *19th Conference on IIPS, Session 15, Application in Meteorology, Oceanography, Hydrology, and Climatology, Part II*. Silver Spring, MD. NOAA.
- NASA-Oak Ridge National Laboratory. 2014. "FLUXNET - A Global Network: Introduction." <http://fluxnet.ornl.gov/introduction> (Accessed June 30, 2016).
- National Climatic Data Center. 2014. "About the Precipitation Analysis Pages." <http://water.weather.gov/precip/about.php> (Accessed June 30, 2016).

- New Mexico State University. 1982. "Jornada Basin LTER: Home." <http://jornada.nmsu.edu/lter> (Accessed June 30, 2015).
- Saha, S., S. Moorthi, H. Pan, X. Wu, J. Wang, S. Nadiga, and R. Reynolds. 2010. "The NCEP climate forecast system reanalysis." *Bulletin of the American Meteorological Society*. 91 (8): 1015–1057.
- Seo, D. 1999. "Real-time estimation of rainfall fields using radar rainfall and rain gauge data." *Journal of Hydrology*. 208: 37-52.
- Smith, J., D. Seo, M. Baeck, and M. Hudlow. 1996. "An intercomparison study of NEXRAD precipitation estimates." *Water Resources Research*. 32 (7): 2035-2045.
- Sorooshian, S., K. Hsu, X. Gao, H.V. Gupta, B. Imam, and D. Braithwaite. 2000. "Evaluation of PERSIANN system satellite-based estimates of tropical rainfall." *Bulletin of American Meteorology Society*. 81: 2035-2046.
- Sorooshian, S., K. Hsu, B. Imam, and Y. Hong. 2005. "Global precipitation estimation from satellite image using artificial neural networks." *Journal of Applied Meteorology*. 36 (2005): 1176-1190.
- University of New Mexico. 1994. "Sevilleta Long Term Ecological Research (LTER) Program: Home." <http://sev.lternet.edu/> (Accessed June 30, 2016).
- University of Oregon. 2015. "Descriptions of PRISM Spatial Climate Datasets for the Conterminous United States: Last Revised July 2015." [http://www.prism.oregonstate.edu/documents/PRISM\\_datasets.pdf](http://www.prism.oregonstate.edu/documents/PRISM_datasets.pdf) (Accessed September 14, 2015).
- Verdin, J., C. Funk, G. Senay, and R. Choularton. 2005. "Climate science and famine early warning." *Philosophical Transactions of the Royal Society B*. 360: 2155–2168.
- Wilson, J. and E. Brandes. 1979. "Radar measurement of rainfall-A summary." *Bulletin of the American Meteorological Society*. 60 (9): 1048-1058.

## APPENDIX A. DEFINITIONS

Algorithm – A self-contained process or set of rules to be followed in calculations or other problem-solving operations, especially by a computer.

Bias - A systematic error or unfair sampling of a population that does not give accurate results on average.

Centroid – The geometric center of a shape.

Chaco Canyon, New Mexico – A remote canyon in the San Juan Basin of northwestern New Mexico, surrounded by the Chuska Mountains to the east, the San Juan Mountains to the north and the San Pedro Mountains to the east. Extremely arid, it is bisected by the Chaco Wash that rarely contains water and was the major cultural center of the Ancient Pueblo Peoples from AD 900 to 1150.

Climatologically-Aided Interpolation – (CAI) Process that takes datasets built from long-term average precipitation measurements to serve as predictor grids. The spatial patterns of climatic conditions for a given month or day are determined by this long-term average pattern.

Comma Delimitation – Separation of numerical values or tabular data by commas in a text file for use in a spreadsheet or application that groups data.

Correlation Scatter Plot – Mathematical diagram using Cartesian coordinates to display values for two variables of data with a certain confidence interval. Relationships between the two variables can have a positive (i.e. rising slope) or negative (i.e. falling slope) correlation denoted by a line of best fit (i.e. a linear regression trend line). A 1:1 correlation (i.e. positive) indicates that for each value in one variable, the same value exists for the other variable.

Data Symmetry – The shape of the data representation in a histogram. In physical science, data that most often occurs in nature is normally distributed and has a symmetrical, classic bell shaped curve. Non-symmetrical and bimodal data indicate multiple or imbalanced forces.

Detrending – Method that subtracts the mean or best-fit line from the data to enable focus of analysis on fluctuations in the data around the trend. A linear trend typically indicates a systematic increase or decrease in the data. A systematic shift can result from sensor drift, for example. While trends can be meaningful, some types of analyses yield better insight once the trends are removed.

Digital Elevation Model – (DEM) A digital, three-dimensional representation of a terrain's surface created from elevation data. Usually represented as a raster or vector-based triangular irregular network and acquired through remote sensing or land surveying.

El Niño – Southern Oscillation – (ENSO) A periodic variation in winds and sea surface temperature over the tropical eastern Pacific Ocean affecting much of the climate across the tropics and subtropics. A warming phase with high air surface pressure (i.e. El Niño) and a cooling phase with low pressure (i.e. La Niña) is coupled with the atmospheric component and sea temperature change (i.e. Southern Oscillation) to cause major precipitation fluctuations from 60°N to 45°S latitudes.

Evapotranspiration – (ET) Sum of the evaporation and plant transpiration from the surface of the land and waterbodies to the atmosphere. Evaporation moves water vapor from soil and water into the atmosphere. Transpiration moves water vapor from plants through stomata in leaves.

Geotiff – A tagged image file format (TIFF) with embedded data that allows the raster to be georeferenced. These files can potentially contain map projections, coordinate systems, ellipsoids, datums and other data to allow exact spatial referencing of all data values.

Geodatabase – (GDB) A collection of various types of geographic datasets (e.g. point, line, or shape features, rasters) useable in ArcGIS held as tables in a common file system folder, Microsoft Access database, or a multiuser relational database management system.

Header – Supplemental data placed at the beginning of a block of graphical data providing information about image size, resolution, data organization and position, and so forth.

Histogram – A graphical representation of the distribution of numerical data providing an idea of the probability that a value will fall within a certain interval. Performed by dividing the entire range of values into a series of intervals and counting how many values fall in each interval.

Hydrologic Unit Code – (HUC) A hierarchical sequence of unique numbers developed by the U.S. Geological Survey to identify drainage areas. Each 2-digit portion of the unit code indicates a smaller division: from a 2-digit region covering the drainage system of an entire river basin to a 12-digit subwatershed covering the drainage of a single fork. For example, **130301020101** = **13**: Rio Grande Region, **03**: Rio Grande-Mimbres Subregion, **01**: Rio Grande-Caballo Basin, **02**: El Paso-Las Cruces Subbasin, **01**: Unnamed Watershed, **01**: Unnamed Subwatershed. HUC8 has 8 digits and is the smallest division used in this project.

Interpolation – A method of constructing new data points within a range of known data points by developing a mathematical equation that has a solution for the known data and solving it for the unknown data. Linear interpolation is the easiest interpolation technique, which draws a straight line between points and solves for unknowns along the line based on the slope. Polynomial interpolation is more complicated looking at degrees of change along a curved line to mimic variable forces.

Kriging – Method of geostatistical interpolation where the interpolated values are modeled on the Gaussian (i.e. normal distribution) regression function governed by the measure of how two variables change together (i.e. covariance). Kriging is a multistep process that includes exploratory statistical analysis of data, modeling spatial continuity of data (i.e. variogram), creating a statistical surface, and exploring the variance of the surface.

MatLab – Short for Matrix Laboratory developed by MathWorks, is a numerical computing environment and programming language allowing matrix manipulations, plotting of functions, implementation of algorithms, and creation of user interfaces that connect to programs written in other languages, such as C, C++, Java, Fortran, and Python.

Metadata – Set of data that provides structural or descriptive information about other data. Metadata is most often used to catalog data for use in organization and discovery based on usefulness and standards specific to a field are included to focus on pertinent information.

Modal – In statistics, the mode is the value occurring with the highest frequency. In a histogram, this value will have the longest bar or highest peak. A multimodal distribution has two or more peaks and indicates forces or occurrences that have multiple variables.

New Mexico Experimental Program to Stimulate Competitive Research – (NM EPSCoR) A state organization made up of faculty and students from state universities and colleges and funded by the National Science Foundation (NSF) to build the state's capacity to conduct scientific research. <https://www.nmepscor.org/>

New Mexico Water Conference – A convention hosted by the New Mexico Water Resources Research Institute to bring the community together each year to discuss critical issues concerning the state's water resources.

Polygon – A two-dimensional, enclosed area of a variety of shapes and sizes, made of vertices (i.e. corners) and edges (i.e. sides).

Precipitation – Any product of the condensation of atmospheric water vapor (e.g. drizzle, rain, sleet, snow, graupel, hail) that falls to the ground under gravity. Precipitation occurs when a portion of the atmosphere becomes saturated with water vapor, so that the water condenses and "precipitates."

Projection – The systematic transformation of the latitudes and longitudes of locations on the surface of a sphere or ellipsoid to locations on a planar surface. Each projection distorts at least one of the following properties and can generally only keep one or two accurate: area, bearing, direction, distance, scale and shape. Tangent (i.e. plane just touching surface) and secant (i.e. plane cutting through surface) lines represent areas of the least distortion.

Raster – A graphic image with a dot matrix data structure representing a generally rectangular grid of pixels or points of color that are viewable on a monitor, sheet of paper, or some other medium. Each data point represented by a pixel of varying sizes (i.e. resolution) has a value with a magnitude that corresponds to a specific viewable color. A set of pixels in a raster is able to display continuous data across a planar surface, such as imagery, elevation, precipitation, evapotranspiration, cloud cover, etc.

Regression – A statistical process for estimating relationships among variables. Many techniques are available for modeling and analyzing several variables focusing on the relationship between a dependent variable and one or more independent variables (i.e. predictors). The process is widely used for prediction and forecasting and with caution, can be used to infer causal relationships.

Remote Sensing – The acquisition of information about an object or phenomenon without making physical contact or being in close proximity. In modern usage, it refers to the use of aerial or orbital sensor technology to detect and classify objects on Earth by means of active (e.g. radar, lidar, sonar) or passive (e.g. sunlight) propagated signals (e.g. electromagnetic radiation, sound).

Root Mean Square Error – (RMSE) The measure of differences between values (sample and population) predicted by a model or an estimator and the values actually observed. The individual differences are called residuals when calculations are performed within the sample used for estimation and prediction errors when calculated out of sample. RMSE is a good measure of accuracy against single variables as it aggregates the magnitudes of the errors in the predictions into a single measure of predictive power.

Shapefile – A geospatial vector data format developed by ESRI for geographic information system software. The “file” consists of a collection of files with a common filename prefix stored in the same directory. This collection stores rows of one type of geometric shape (e.g. points, lines, polygons), fields of attributes about each shape, projection information used to locate each shape, spatial indices to optimize location queries, and metadata about the shapes. Shapefiles lack the capacity to store topological rules, so shapes can overlap without error

Steppe Environment – An ecoregion characterized by grassland plains without trees apart from those near waterbodies. It may be semi-desert, or covered with grass or shrubs or both, depending on the season and latitude. It has a climate in regions too dry to support a forest, but not dry enough to be a desert

Symbology – A set of conventions, rules, or encoding systems that define how geographic information is represented with colors, sizes and shapes of symbols on a map. Organized collections of symbols and colors are generally included in map legends.

Thermohaline Circulation – Part of the large-scale ocean circulation driven by density gradients created by surface heat and freshwater fluxes. Both temperature and salt content determine the density of sea water, which in turn determines its flow characteristics. Wind-driven surface currents move seawater poleward from the equator, where it cools, sinks and eventually resurfaces, circulating energy and matter around the globe.

Time Series – A series of data points listed or graphed in time order to be used in statistics, pattern recognition, engineering, prediction and forecasting. An analysis of time series data uses a model to predict future values based on previously observed values.

Water Budget – Also called water balance in hydrology, is an equation used to describe the flow of water in and out of a system. The system can be one or many of several hydrological domains, such as waterbodies, groundwater, or columns of soil or atmosphere. The general equation for an area is precipitation - evapotranspiration - streamflow = change in storage.